Short title: Ascorbate deficiency and NPQ in *C. reinhardtii*

Corresponding author:

Szilvia Z. Tóth

ORCID: https://orcid.org/0000-0003-3419-829X

e-mail: toth.szilviazita@brc.mta.hu

Title:

Ascorbate deficiency does not limit non-photochemical quenching in *Chlamydomonas reinhardtii*

Authors:

André Vidal-Meireles[1], Dávid Tóth[1,2], László Kovács[1], Juliane Neupert[3], Szilvia Z. Tóth[1]*

[1]Institute of Plant Biology, Biological Research Centre, Szeged, Hungary

[2]Doctoral School of Biology, University of Szeged, Szeged, Hungary

[3]Max-Planck Institut für Molekulare Pflanzenphysiologie, Potsdam-Golm, Germany

One-sentence summary:

In contrast to seed plants, ascorbate is not required for violaxanthin deepoxidation and energy-dependent non-photochemical quenching, but it mitigates photoinhibitory quenching in *C. reinhardtii*.

Footnotes:

Author contributions: A. V.-M., J. N. and D. T. characterized the *Crvtc2-1* mutant and generated the complementation lines. L. K. developed the carotenoid content determination method. A. V.-M. performed the chl *a* fluorescence measurements, immunoblot analyses, and ascorbate content measurements. S. Z. T. conceived the study, analyzed the data and wrote the paper. A. V.-M. L. K. and J. N. contributed to analyzing the data and to writing the paper.

Funding:

This work was supported by the Lendület/Momentum Programme of the Hungarian Academy of Sciences (LP-2014/19), the National, Research and Development Office (NN 114524, GINOP-2.3.2-15-2016-00026) and the Alexander von Humboldt Foundation (grants to S Z T). A V-M received fellowships from the SEB / Company of Biologists Travel Fund, US DOE Travel Award and from the International Society of Photosynthesis Research (sponsored by Wiley on behalf of Plant, Cell and Environment).

Email address of author for contact:

toth.szilviazita@brc.hu (Szilvia Z. Tóth)

Abstract

Ascorbate (Asc, vitamin C) plays essential roles in development, signaling, hormone biosynthesis, regulation of gene expression, stress resistance and photoprotection. In vascular plants, violaxanthin de-epoxidase (VDE) requires Asc as reductant, thereby it is required for the energy-dependent component of non-photochemical quenching (NPQ). To assess the role of Asc in NPQ in green algae, which are known to contain low amounts of Asc, we searched for an insertional *Chlamydomonas reinhardtii* mutant affected in the *VTC2* gene encoding GDP-L-galactose phosphorylase, which catalyzes the first committed step in the biosynthesis of Asc.. The *Crvtc2-1* knockout mutant was viable and, depending on the growth conditions, contained 10 to 20% Asc relative to its wild type. When *C. reinhardtii* was grown photomixotrophically at moderate light, the zeaxanthin-dependent component of NPQ emerged upon strong red illumination both in the *Crvtc2-1* mutant and in its wild type. Deepoxidation was unaffected by Asc deficiency, demonstrating the Chlorophycean VDE found in *C. reinhardtii* does not require Asc as a reductant. The rapidly induced, energy-dependent NPQ component characteristic of photoautotrophic *C. reinhardtii*cultures grown at high light was not limited by Asc deficiency either. On the other hand, a reactive oxygen species-induced photoinhibitory NPQ component was greatly enhanced upon Asc deficiency, both under photomixotrophic and photoautotrophic conditions. These results demonstrate Asc has distinct roles in NPQ formation in *C. reinhardtii*than in vascular plants.

Introduction

Ascorbate (Asc) is a multifunctional metabolite essential for a range of cellular processes in green plants, including cell division, stomatal movement, biosynthesis of various plant hormones, epigenetic regulation and reactive oxygen species (ROS) scavenging (Asada, 2006; Foyer and Shigeoka, 2011; Smirnoff, 2018). Within the chloroplast, Asc may also act as an alternative electron donor to photosystem II (PSII) and to PSI (Ivanov et al., 2007; Tóth et al., 2009; Tóth et al., 2011). In vascular plants, violaxanthin de-epoxidase (VDE) requires Asc as reductant, thereby Asc plays an essential role in the process of non-photochemical quenching (NPQ) to dissipate excess energy as heat (Bratt et al., 1995; Saga et al., 2010; Hallin et al., 2016).

To fulfill the multiple physiological roles of Asc (reviewed by Tóth et al., 2018; Smirnoff, 2018), vascular plants maintain their Asc concentration at a high, approximately 20 to 30 mM level (Zechmann et al., 2011), which is also relatively constant, usually with no more than two-fold increases upon stress treatments and moderate decreases during dark periods (Dowdle et al., 2007). Notwithstanding, Asc concentration may be limiting under environmental stress conditions, as shown by increased oxidative stress tolerance of plants overexpressing dehydroascorbate reductase, essential in Asc regeneration (Wang et al., 2010). Asc-deficient Arabidopsis (*Arabidopsis thaliana*) plants have slowly inducible and diminished NPQ, whereas Asc-overproducing plants possess enhanced NPQ relative to wild-type plants, indicating Asc may limit the conversion of violaxanthin to zeaxanthin *in vivo* (Müller-Moulé et al., 2002; Tóth et al., 2011). Asc-deficient plants are also sensitive to high light, especially in combination with zeaxanthin deficiency (Müller-Moulé et al., 2003).

Green algae, such as *Chlamydomonas reinhardtii*, produce Asc in small amounts under favorable environmental conditions (approx. 100 to 400 µM, Gest et al., 2013) and

boost Asc levels only in case of need, for instance upon a sudden increase in light intensity and in nutrient deprivation (Vidal-Meireles et al., 2017; Nagy et al., 2018). Regulation of Asc biosynthesis differs largely between plants and *C. reinhardtii*: in contrast to vascular plants, i) green algal Asc biosynthesis is directly regulated by ROS, ii) it is not under circadian clock control and, iii) instead of a negative feedback regulation, there is a feedforward mechanism on the expression of the key Asc biosynthesis gene, *VTC2* (*Cre13.g588150*, encoding GDP-L-galactose phosphorylase) by Asc in the physiological concentration range (Vidal-Meireles et al., 2017).

VDE found in Chlorophyceae (CVDE) is not homologous to plant VDE but related to a lycopene cyclase of photosynthetic bacteria (Li et al., 2016a). *C. reinhardtii* CVDE (CrCVDE), encoded by *Cre04.g221550*, has a FAD-binding domain and is located on the stromal side and not in the thylakoid lumen, as it is the case for plant-type VDE (Li et al., 2016a). The cofactor or reductant requirement of the CrCVDE enzyme has not been investigated, and it is not known whether its activity requires Asc, either directly or indirectly.

Due to the major differences in Asc contents, the regulation of Asc biosynthesis and the VDE enzymes of vascular plants and Chlorophyceae, we decided to assess the role of Asc in the various NPQ components in *C. reinhardtii*. To this end, we characterized an insertional *VTC2* mutant procured from the CLiP library (Li et al., 2016b), possessing only 10 to 20% Asc relative to its parent strain. We have found, in contrast to vascular plants, Asc deficiency does not limit energy-dependent quenching (qE) and violaxanthin de-epoxidation in *C. reinhardtii*; instead, Asc deficiency leads to enhanced photoinhibitory quenching (qI) upon excessive illumination.

Results

Identification and initial characterization of an Asc-deficient VTC2 *insertional mutant of* C. reinhardtii *and its genetic complementation*

To investigate the function of Asc in NPQ in *C. reinhardtii*, we searched for insertion mutants of *VTC2* in the CLiP library (Li et al., 2016b). We found one putative *VTC2* mutant (strain LMJ.RY0402.058624, hereafter called *Crvtc2-1* mutant), holding one insertion of the paromomycin resistance (CIB1) casette at the junction site of exon 3 and the adjacent upstream intron of *VTC2* (Fig. 1A). The other available mutants were affected in the 3'UTR region of *VTC2* and/or had multiple insertions in genes other than *VTC2* thus were found unsuitable for this study. Due to the lack of another, independent CIB insertional mutant line affecting only *VTC2*, we carried out several NPQ measurements on our previously published *VTC2*-artificial microRNA (amiRNA) line (Vidal-Meireles et al., 2017) to confirm our findings on the consequences of Asc deficiency on NPQ (see below).

The site of CIB1 casette integration in the CLiP mutants had been validated by LEAP-Seq method (Li et al., 2016b), and we verified the insertion site in the *Crvtc2-1* mutant by PCR (Fig. 1B). Using primers annealing upstream the predicted insertion site in *VTC2*, a specific 852 bp fragment was observed in genomic DNA samples isolated from wild-type *C. reinhardtii* cells (CC-4533) and from the *Crvtc2-1* mutant strain (Fig. 1B, top panel); using primers designed to amplify the 5' and 3' junction sites of the CIB1 cassette, specific 470 and 601 bp fragments could be detected in the *Crvtc2-1* mutant (Fig. 1B, middle and bottom panels). Sequencing analysis of the PCR amplicons confirmed the predicted insertion of the CIB1 cassette in antisense orientation with its 5' junction in the third exon of the gene and the 3' junction reaching to the adjacent intron upstream of exon 3 (Supplemental Fig. S1).

Under moderate light (100 µmol photons m^{-2} s^{-1}) and photomixotrophic conditions (growth in Tris-acetate-phosphate (TAP) medium), the wild-type strain (CC-4533) had

approx. 12 pmol Asc/ µg Chl(a+b) (Fig. 1C), corresponding to about 200 µM cellular Asc concentration (see Kovács et al., 2016 for calculations), and the *Crvtc2-1* mutant had an Asc content only approx. 10% of the wild type. When the cultures were treated with 1.5 mM H_2O_2, which results in a strong increase in Asc content (Urzica et al., 2012; Vidal-Meireles et al., 2017), the Asc content in the wild type increased approximately three-fold, whereas it did not increase in the *Crvtc2-1* mutant (Fig. 1C). This is in contrast to the *VTC2*-amiRNA lines generated earlier, where H_2O_2 treatment resulted in noticeable Asc accumulation (Vidal-Meireles et al., 2017).

RT-qPCR analysis with primers located upstream and downstream of the insertion site of the CIB1 cassette did not detect*VTC2* transcripts in the *Crvtc2-1* mutant samples grown under normal growth conditions or treated with H_2O_2 (Fig. 1D). Similarly, RT-PCR analysis using primers spanning the sequence encoding the catalytic site of *VTC2* (which is located downstream of the CIB1 casette insertion site) did not detect transcripts in the *Crvtc2-1* mutant under normal growth conditions, and only a weak signal was observed upon 35 PCR cycles in the H_2O_2-treated *Crvtc2-1* mutant samples (Fig. 1E).

To confirm the decrease in Asc content was caused by the functional deletion of *VTC2* in the insertional mutant strain, we performed genetic complementation. To this end, we transformed the *Crvtc2-1* insertional mutant with the coding sequence of *VTC2* controlled by the constitutive promoter *PsaD*. The plasmid used for transformation included the *APH7"* resistance gene (Fig. 2A), thus the ability to grow on a medium containing hygromycin-B was used as the first screening method for successful transformation.

The integration of the plasmid in the genome was verified by PCR. Using a forward primer annealing to the *PSAD* promoter region and a reverse primer annealing to the 5' end of the *VTC2* coding sequence, a specific 841 bp fragment was amplified in genomic DNA samples isolated from two independent complementation lines of *Crvtc2-1+VTC2* (Fig. 2B).

The *VTC2* transcript was detected in the complemented *Crvtc2-1+VTC2* lines via RT-PCR analysiswith primers spanning the sequence encoding the catalytic site (Fig. 2C). The Asc content of the complementation lines was considerably restored (Fig. 2D). The cell volume, the cellular Chl content and Chl*a/b* ratios were moderately increased in the *Crvtc2-1* mutant relative to the wild type, and these parameters were partially restored upon complementation (Supplemental Fig. S2A, B, C).

No significant difference was observed in growth phenotypes between the strains when grown in TAP medium at 100 µmol photons m^{-2} s^{-1}, whereas the growth of the *Crvtc2-1* mutant was severely inhibited in TAP medium at 530 µmol photons m^{-2} s^{-1}, which was restored upon genetic complementation. In high salt (HS) medium at 530 µmol photons m^{-2} s^{-1} growth was slow in all genotypes, and no significant differences were observed among them (Supplemental Fig. S2D). The Asc content increased two- to three-fold in each strain upon high light treatment, and the Asc content of the *Crvtc2-1* mutant remained at a level of 10-20% relative to the wild type and the complementation lines (Supplemental Fig. S2E).

The effects of Asc deficiency on NPQ in cultures grown at normal light and photomixotrophic conditions

NPQ includes short-term responses to changes in light intensity, as well as responses that occur over longer periods allowing for acclimation to high light exposure. In *C. reinhardtii*, the levels of the different NPQ components are variable and highly dependent on the growth conditions (Niyogi et al., 1997; Finazzi et al., 2006; Iwai et al., 2007; Peers et al 2009).

In a first set of experiments to assess the effects of Asc deficiency on NPQ, *C. reinhardtii* strains were cultured in TAP medium at 100 µmol photons m^{-2} s^{-1}. Before the NPQ measurements, cultures were dark-adapted for about 30 min with shaking to avoid anaerobiosis; this dark adaptation protocol ensures the relaxation of most NPQ processes and

the separation of the NPQ components induced under high light illumination (Roach and Na, 2017). When subjecting the cells to continuous red light of 530 µmol photons m^{-2} s^{-1}, a small, rapidly induced NPQ component was induced in the wild type and the Asc-deficient *Crvtc2-1* strain in the first 2 min (Fig. 3A) that we attribute to qE. qE is activated by low lumen pH, which occurs, for instance, during the induction of photosynthesis and upon CO_2 limitation of the Calvin-Benson-Bassham cycle (Kanazawa and Kramer, 2002; Takizawa et al., 2008). In *C. reinhardtii*, qE formation also requires zeaxanthin or lutein (Ericksson et al., 2015) and is enhanced by a stress-related LHC protein, LHCSR3, which is strongly expressed when algae are grown at high light (Xue et al., 2015; Peers et al., 2009; Bonente et al., 2011; Chaux et al., 2017). At moderate light (100 µmol photons m^{-2} s^{-1}) and photomixotrophic growth conditions, the LHCSR3 level was relatively low, particularly in the *Crvtc2-1* strain (Supplemental Fig. S3). The presence of acetate also enables high Calvin-Benson-Bassham cycle activity and a relatively low qE (Johnson and Alric, 2012), in agreement with our findings.

A slower NPQ component, induced on the timescale of several minutes, was also present, which was enhanced in the Asc-deficient *Crvtc2-1* mutant (Fig. 3A) and restored in its complementation strains (Supplemental Fig. S4A). This slow component was enhanced in our previously published *VTC2*-amiRNA line relative to its control strain as well (Supplemental Fig. S4C).

Three components may be responsible for this slowly induced NPQ component (see Ericksson et al., 2015; Allorent et al., 2013): i) zeaxanthin-dependent quenching, which may act on NPQ directly (e.g. Holt et al., 2005; Holub et al., 2007; Avenson et al., 2008) or indirectly by controlling the sensitivity of qE to the pH gradient or promoting conformational changes within LHCs (e.g. Johnson et al., 2008; Ruban et al., 2012); ii) State transition-dependent quenching (qT), which may contribute to balancing excitation energy between

PSII and PSI via LHCII phosphorylation and antenna dissociation from PSII (Depège, 2003; Lemeille et al., 2009; Ünlü et al., 2014); iii) A slowly relaxing, "photoinhibitory" quenching (qI), associated with photosystem II (PSII) damage or slowly reversible downregulation of PSII representing a continuous form of photoprotection (Adams et al. 2013; Tikkanen et al., 2014).

To decipher the origin of the slow NPQ component and to study the possible role of Asc in NPQ, carotenoids were analyzed first using HPLC. Upon illumination, the de-epoxidation index largely increased (from about 0.05 to 0.25) both in the CC-4533 (wild type) strain and the *Crvtc2-1* mutant, and de-epoxidation only moderately recovered after the cessation of actinic illumination in both strains (Fig. 3B). Violaxanthin, antheraxanthin and zeaxanthin concentrations were essentially the same in the *Crvtc2-1* mutant and in the wild type (Supplemental Fig. S5A, B, C). These results suggest qZ was partially responsible for the slow NPQ component and Asc deficiency does not limit the de-epoxidation reaction. We also found the amounts of β-carotene and lutein were not affected by the lack of Asc and their quantities remained constant during the entire protocol (Supplemental Fig. S5D, E). The F_V/F_M values of dark-adapted cultures and those subjected to high light illumination followed by a recovery period were also very similar, with no major differences between the Asc-deficient mutant and the CC-4533 strain (Fig. 3C).

Since the de-epoxidation ratios were the same in the CC-4533 strain and in the *Crvtc2-1* mutant (Fig. 3B), it is likely Asc-deficiency does not limit the reaction. To completely exclude this possibility, a 16-h dark acclimation experiment was conducted, ensuring undetectably low levels of Asc (Fig. 4A). Still, NPQ was induced slowly upon illumination (Fig. 4B), and the de-epoxidation indices were similar than in cultures subjected to relatively short dark adaptation (compare Fig. 4C and Fig. 3B); we note that during a 30-min illumination Asc does not accumulate (Vidal-Meireles et al., 2017).

The large increase in the de-epoxidation index upon illumination suggests qZ is at least partially responsible for the slow NPQ component. However, we also observed the slow NPQ component was larger in the *Crvtc2-1* mutant than in the wild type, whereas the de-epoxidation ratios were the same (Fig. 3A, B). In addition to qZ, qT and qI mechanisms may also contribute to the slow component, and they may differ between the wild type and the *Crvtc2-1* mutant. The possible contribution of qT was studied by measuring 77K fluorescence spectra: Upon illumination with 530 µmol photons $m^{-2}s^{-1}$ red light, the 684 nm/710 nm ratio remained unaltered in the wild type and increased slightly in the Asc-deficient mutant (Fig. 3D). Transition from state I to state II would decrease the 684/710 nm ratio; therefore, in our cultures grown at moderate light in TAP medium and subjected to strong red illumination during the fluorescence measurement, qT is unlikely to contribute to NPQ induction. On the other hand, when the actinic illumination was switched off, the 684/710 nm ratio decreased moderately, reflecting the occurrence of state I to state II transition in the dark.

To further study the effect of state transition in the induction and relaxation of NPQ, we employed a state transition mutant, called *stt7-9* (Depège et al., 2003). NPQ was induced during illumination in the *stt7-9* mutant to a similar extent as in the *Crvtc2-1* mutant (albeit with rather different kinetics), which coincided with a strong zeaxanthin accumulation (Supplemental Fig. S6B); this indicates transition to state II did not play a role in the formation of NPQ under the present experimental conditions. On the other hand, upon the cessation of actinic illumination, there was a rapid NPQ relaxation in the *stt7-9* mutant, showing transition to state II occurs in the wild types and the *Crvtc2-1* mutant in the dark, probably masking the relaxation of the other NPQ components.

As a next step, the effect of oxidative stress, known to enhance NPQ (Roach and Na, 2017), was tested by employing H_2O_2 and catalase treatments on the *Crvtc2-1* mutant and its

wild type. Fig. 5A and B show that upon the addition of 1.5 mM H_2O_2, the slow NPQ component increased remarkably in both strains, without altering the de-epoxidation level (Fig. 5C). When 5 µg/ml catalase was added, NPQ was only slightly affected in the wild type (Fig. 5D), whereas it significantly decreased in the Asc-deficient mutant (Fig. 5E). These data suggest H_2O_2 accumulated upon strong illumination in the Asc-deficient mutant, resulting in enhanced NPQ. On the other hand, the F_V/F_M value, an indicator of photosynthetic efficiency, did recover following illumination and to a similar extent in the wild type and the *Crvtc2-1* strain (Fig. 3C), thus photosynthetic reaction centers were not severely inhibited.

For comparison, we also tested the *npq1* mutant lacking the CVDE enzyme, thus unable to perform violaxanthin de-epoxidation (Niyogi et al., 1997). Upon illumination with 530 µmol photons m^{-2} s^{-1}, this strain developed a large NPQ (Fig. 6A), which was accompanied by an irreversible decrease of F_V/F_M and loss of Chl and β-carotene relative to its wild type (137a) strain (Fig. 6B, C, D). 77 K fluorescence recordings showed no changes in the 684nm/710nm ratio (Fig. 6E), thus the large NPQ component could be unambiguously attributed to photoinhibitory qI. Interestingly, the Asc concentration in the *npq1* mutant was very high compared to the other strains (Fig. 6F), probably to compensate for the lack of CVDE and zeaxanthin in ROS management (Baroli et al., 2003). Thus, the experiments on the *npq1* mutant corroborate the importance of CVDE in strong illumination.

The effects of Asc deficiency on NPQ in cultures grown under photoautotrophic conditions at high and moderate light

When the cultures were grown under photoautotrophic conditions without CO_2 supplementation under strong white light (530 µmol photons $m^{-2}s^{-1}$), which was similar in intensity used for NPQ induction measurements, qE reached relatively high values (about 1.0) both in the wild type and the Asc-deficient CLiP mutant (Fig. 7A). In the *VTC2*-amiRNA

line, the qE component was enhanced relative to its empty vector control (Supplemental Fig. S4D). These results show Asc is not required for the formation of the qE component. The qE phase was followed by a slower one, which was enhanced both in the *Crvtc2-1* mutant and the *VTC2* amiRNA line relative to their control strains.

During illumination, the de-epoxidation index changed only marginally, and it was essentially the same in the wild type and in the Asc-deficient strain (about 0.1, Fig. 7B). The F_V/F_M value was also unaffected in the *Crvtc2-1* mutant relative to its wild type before or after the illumination with strong red light (Fig. 7C). The 684nm/710nm ratio of the 77 K spectra remained constant in the Asc-deficient mutant (Fig. 7D). The violaxanthin, antheraxanthin, zeaxanthin and lutein contents did not decrease upon illumination with intense red light in either strain (Supplemental Fig. S7), only the total amount of β-carotene was slightly lower in the Asc-deficient mutant (Supplemental Fig. S7D). We also observed that under high light growth conditions, the amount of photosynthetic complexes (namely PsbA, CP43, PSBO, PsaA, LHCSR3, PetB and RbcL) were essentially the same in the *Crvtc2-1* mutant and in the wild type, as detected by immunoblot analysis on equal chl basis (Supplemental Fig. S3).

Treatments with 1.5 mM H_2O_2 led to alteration of the NPQ kinetics and a slower relaxation in both strains (Fig. 8A, B). In the *Crvtc2-1* mutant, catalase treatment resulted in a strong decrease of qE and the slow NPQ component (Fig. 8C, D). These results show that under photoautotrophic and high light conditions, Asc-deficiency does not limit qE or qZ but may lead to the occurrence of oxidative stress and thereby to increased qI.

Subjecting the cells in HS medium to moderate light (100 µmol photons $m^{-2}s^{-1}$) resulted in similar effects in terms of qE, de-epoxidation, the 684/710 nm ratio of the 77 K spectra and H_2O_2 and catalase responsiveness (Supplemental Fig. S8).

Discussion

The Crvtc2-1 CLiP mutant possesses a low Asc content without major changes in the phenotype

VTC2 encodes GDP-L-galactose phosphorylase, an essential and highly regulated enzyme of Asc biosynthesis both in vascular plants and in green algae (Urzica et al., 2012; Vidal-Meireles et al., 2017), and downregulating *VTC2* via the amiRNA technique results in Asc deficiency (Vidal-Meireles et al., 2017). For the present study, we identified and genetically complemented a *VTC2* mutant in the CLiP collection that carries a single insertion in the *VTC2* gene (Fig. 1 and Fig. 2). Asc content in the *Crvtc2-1* mutant was about 10% of its wild-type strain CC-4533 under normal growth conditions, was unaltered upon H_2O_2 treatment and remained below 20% of the wild type under high light conditions; in addition, by employing overnight dark acclimation, the Asc concentration of the *Crvtc2-1* mutant strongly decreased (Fig. 4).

The *Crvtc2-1* mutant is likely a knockout for *VTC2* as no transcript accumulation was detected when performing RT-PCR with primers annealing downstream of the CIB cassette insertion site and spanning the sequence encoding the catalytic site of GDP-L-galactose phosphorylase. A faint band could only be observed in the gel when the cultures were treated with H_2O_2 and when a high PCR cycle number was used (Fig. 1E). It is very unlikely a functional truncated GDP-L-galactose phosphorylase is present in the mutant, but the observation that the *Crvtc2-1* strain still contains 10-20% Asc relative to its parent strain suggests some phosphorolysis of GDP-L-galactose could be carried out by another enzyme ensuring a minor amount of Asc. We note that in Arabidopsis *VTC2* has a lowly expressed homologue, *VTC5*, and knocking out both of them results in seedling lethality (Dowdle et al., 2007). In *C. reinhardtii*, no homologue of *VTC2* has been identified (Urzica et al., 2012). On

the other hand, it is possible GDP-L-galactose is degraded hydrolytically (with L-galactose-1-P and GMP as products) leading to minor Asc production in the *VTC2* mutant. An alternative Asc biosynthesis pathway may also exist in *C. reinhardtii*, although homologues of enzymes possibly involved in alternative Asc biosynthesis pathways in vascular plants could not be found in *C. reinhardtii* (Urzica et al., 2012; Wheeler et al., 2015).

In spite of the very low Asc content of the *Crvtc2-1* mutant, the phenotype was only moderately altered. The *Crvtc2-1* mutant had the same growth rate as the wild type and the complementation lines at moderate light conditions in TAP medium (Supplemental Fig. S2). The amounts of various photosynthetic subunits were similar in the Asc-deficient *Crvtc2-1* mutant than in the wild type strain CC-4533 in TAP medium at moderate light and also in HS medium both at moderate and high light (Supplemental Figure S3). Unexpectedly, the amount of the photoprotective LHCSR3 protein was reduced in the *Crvtc2-1* mutant in TAP medium at moderate light and was the same level as in the wild type when grown in HS medium both at medium and high light. The amounts of carotenoids were unchanged in the *Crvtc2-1* line in cultures grown at normal light, whereas at high light in HS medium, the amount of β-carotene was slightly reduced (Supplemental Fig. S5 and S7). The *Crvtc2-1* line had a slightly higher Chl content and moderately larger cell size than its wild type (Fig. 2). A marked characteristic of the *Crvtc2-1* mutants was that it was unable to grow at high light in TAP medium (Supplemental Fig. S2).

In our previously published *VTC2*-amiRNA line, Asc deficiency led to more severe alterations in the phenotype than was observed in the *Crvtc2-1* mutant (Vidal-Meireles et al., 2017). The reason behind this remains to be elucidated, although the cell wall deficiency of the cw15-325 line (the parent strain of the *VTC2*-amiRNA line) and thereby its increased stress sensitivity (Voigt and Münzner, 1994) may explain the differences between the *VTC2*-amiRNA and the *Crvtc2-1* insertional mutant strains.

The effects of Asc deficiency on the qE component of NPQ

C. reinhardtii uses various photoacclimation strategies which strongly depend on carbon availability and trophic status of the cells (Polukhina et al., 2016). The fast rise in NPQ (qE) is enhanced upon growth at high light and low CO_2 that is enabled by a high expression of LHCSR3 (e.g. Peers et al., 2009). Under photomixotrophic conditions at normal light, the expression of the LHCSR proteins is very low and qE is minor; in addition, the deepoxidation state also varies with the growth light (Polukhina et al., 2016). Therefore, to study the role of Asc in the different NPQ parameters, we subjected the cultures both to moderate and high light, photomixotrophic and photoautotrophic conditions. As shown by our results and the discussion below, by these means we managed to distinguish between qE, qZ, and qI, and only qT could not be studied in detail.

Rapid response to changes in light intensity and dissipation of excess light energy are particularly important when the activity of the Calvin-Benson-Bassham cycle is limiting to avoid a potentially deleterious buildup of excessive ΔpH (Kanazawa and Kramer, 2002; Takizawa et al., 2008). In agreement with the literature (Xue et al., 2015), at normal light and photomixotrophic conditions, the rapidly inducible qE was a minor component and the relative amount of the LHCSR3 protein, essential for qE development, was low (Supplemental Fig. S3). When *C. reinhardtii* cultures were grown at photoautotrophic, possibly CO_2-limiting conditions, the amplitude of qE largely increased both at moderate and high light (Supplemental Fig S8 and Fig. 8, respectively) enabled by the accumulation of LHCSR3 (Supplemental Fig. S3) and possibly by other factors.

Our results on the *Crvtc2-1* line show qE is not limited by Asc deficiency neither at low light nor at high light conditions, nor under photomixotrophic and photoautotrophic

conditions; in the *VTC2*-amiRNA line, qE was even enhanced relative to its control line (Supplemental Fig. S4B).

The effects of Asc deficiency on the slow NPQ components

In *C. reinhardtii*, a slowly induced NPQ component, with several underlying mechanisms, may also be induced. When CC-4533 cultures were grown at normal light in TAP medium and subjected to strong red light, the major slow component was probably qZ, as shown by the large increase in de-epoxidation (Fig. 3) and by the loss of NPQ induction in the *npq1* mutant (Fig. 6). In cultures grown at high light and photoautotrophic conditions, de-epoxidation was minor upon light adaptation with strong red light (Fig. 7) and intermediate when the cultures were grown photoautotrophically at moderate light (Supplemental Fig. S8). De-epoxidation was equal in the *Crvtc2-1* mutant and the wild type in all growth conditions and also upon overnight dark acclimation that led to undetectably low Asc content in the *Crvtc2-1* mutant. These results clearly show Asc deficiency is not limiting qZ, thus Asc is not used as a reductant by CrCVDE.

The xanthophyll cycle, in which violaxanthin is converted into zeaxanthin during light acclimation, is ubiquitous among green algae, mosses and plants, with exception of Bryopsidales, a monophyletic branch of the Ulvophyceaes in which NPQ is neither related to a pH-dependent mechanism nor modulated by the activity of the xanthophyll cycle (Christa et al., 2017). Among green alga species, large variations exist in the activity of xanthophyll cycle and in its overall contribution to NPQ, which seems to depend on the environmental selection pressure and less on the phylogeny (Quaas et al., 2015). In mosses, the xanthophyll cycle significantly contributes to excess energy dissipation upon stress conditions (e.g. Azzabi et al., 2012).

The de-epoxidation reaction itself is catalyzed by distinct enzymes in vascular plants and in Chlorophyceae, including *C. reinhardtii* (Li et al., 2016a). Plant-type VDE is associated with the thylakoid membrane on the luminal side, where it catalyzes the de-epoxidation reaction of violaxanthin, found in free lipid phase, and uses Asc as a reductant (Hager and Holocher, 1994; Arnoux et al., 2009). CVDE is located on the stromal side of the thylakoid membrane, and, just like vascular plant VDE, it also requires a build-up of ΔpH for its activity (Li et al., 2016a). CVDE is related to lycopene cyclases of photosynthetic bacteria, called CruA and CruP (Li et al., 2016a, Bradbury et al., 2012). We have demonstrated in this paper Asc is not required for the de-epoxidation reaction, and, in general, for qZ in *C. reinhardtii*.

Green algae contain very small amounts of Asc relative to vascular plants, and, as stated above, effective de-epoxidation is achieved by an enzyme that does not require Asc as a reductant. Interestingly, in brown algae, which produce minor amounts of Asc as well, diadinoxanthin de-epoxidase uses Asc as a reductant with much higher affinity for Asc than plant-type VDE, in combination with a shift of its pH optimum towards lower values enabling efficient de-epoxidation (Grouneva et al., 2006). Mosses have plant-type VDE enzymes (Pinnola et al., 2013), which probably require Asc as a reductant. Since mosses contain approx. ten times less Asc compared to vascular plants (Gest et al., 2013), it remains to be explored how this low amount of Asc allows a rapid and intensive development of NPQ, characteric of mosses (e.g. Marschall and Proctor, 2004).

In *C. reinhardtii*, light and O_2 availability-dependent state transitions (qT) involving major reorganizations of LHCs also modulate NPQ (Depège, 2003; Lemeille et al., 2009; Ünlü et al., 2014). Under our experimental conditions, ensuring aeration during both the dark and the light adaptation and using strong red light as actinic light, no decrease occurred in the 685/710 nm ratio of the 77 K fluorescence spectra, suggesting state I to state II transition did

not affect the NPQ induction in the wild type nor in the Asc-deficient strains. The *stt7-9* mutant, which is unable to perform state transition, did not show decreased NPQ (Supplemental Fig. S6), which would be expected if state transition constituted a major form of NPQ under our experimental conditions. However, our data do not exclude the possibility Asc may participate in state transition under conditions favoring its occurrence.

A fourth and rather complex component of NPQ is qI, possibly with several underlying mechanisms involved (Adams et al., 2013; Tikkanen et al., 2014). We observed both under photomixotrophic conditions at moderate light and under photoautotrophic conditions that the slow NPQ component was enhanced in the *Crvtc2-1* mutant upon illumination with strong red light that was not attributable to qZ or to qT. Asc deficiency is accompanied by an increase in the intracellular H_2O_2 content in *C. reinhardtii* (Vidal-Meireles et al., 2017), and ROS are known to enhance NPQ via several mechanisms (Roach and Na, 2017). Using H_2O_2 and catalase treatments (Fig. 5 and 8, Supplemental Fig. S8), we clearly show ROS formation is involved in the slowly induced NPQ component in the Asc-deficient strain that can be interpreted as qI. In the wild type, the contribution of qI to NPQ was probably minor under our experimental conditions, since catalase treatment did not diminish NPQ formation (Fig. 5D).

In conclusion, our results reveal fundamental differences between vascular plants and *C. reinhardtii* regarding the role of Asc in NPQ. Whereas the most prominent role of Asc in vascular plants is a reductant of VDE, it is pertinent in preventing ROS formation that would lead to photoinhibitory quenching mechanisms in *C. reinhardtii*.

Materials and Methods

Algal strains and growth conditions

Chlamydomonas reinhardtii strains CC-4533 (designated as wild type) and LMJ.RY0402.058624 (designated as *Crvtc2-1* mutant) were obtained from the CLiP library (Li et al., 2016b). The 137a (CC-125) strain and the *npq1* (CC-4100) mutant were obtained from the Chlamydomonas Resource Center (https://www.chlamycollection.org/). The *ARG7* complemented strain *cw15-412* (provided by Dr Michael Schroda (Technische Universität Kaiserslautern, Germany)) was used as control for the *stt7-9* mutant (Depège et al., 2003). The *VTC2*-amiRNA strain and its control *EV2* strain are described in Vidal-Meireles et al. (2017).

The synthetic coding sequence of *VTC2* including a 38 bp-long upstream sequence homologous to the *PSAD* 5'UTR with the BsmI restriction enzyme recognition site was ordered from Genecust (www.genecust.com). The *VTC2* insert was ligated as BsmI/EcoRI fragment into the similarily digested pJR39 (Neupert et al., 2009) vector, resulting in vector pJR112. Finally, pJR112 was digested with BsmI and SmaI, and the *VTC2*-containing BsmI/SmaI fragment was ligated to the similarily digested pJR91 vector that carries the *APH7''* resistance marker for selection on hygromycin-B. Transformation of the *Crvtc2-1* mutant strain was done via electroporation in a Bio-Rad GenePulser Xcell™ instrument, at 1000 V, with 10 F capacitance and infinite resistance using a 4-mm gap cuvette. The cells were plated onto selective agar plates (TAP + 10 µg/ml hygromycin-B), and colonies were picked after 10 days of growth under moderate light (80 µmol photons m^{-2} s^{-1}).

C. reinhardtii pre-cultures were grown in 50-ml Erlenmeyer flasks in Tris-acetate phosphate (TAP) medium for three days at 22°C and 100 µmol photons m^{-2} s^{-1} on a rotatory shaker. Following this phase, cultures were grown in 100-ml Erlenmeyer flasks photomixotrophically (in TAP medium) or photoautotrophically (in high salt (HS) medium) at 22°C at 100 or 530 µmol photons m^{-2} s^{-1} for two additional days. The initial cell density was set to 1 million cells/ml.

DNA Isolation and PCR

Total genomic DNA from *C. reinhardtii* strains CC-4533 and *Crvt2-1* (LMJ.RY0402.058624) was extracted according to published protocols (Barahimipour et al., 2015; Schroda et al., 2001), and 1 µl of the extracted DNA was used as template for the PCR assays, using the GoTaq DNA polymerase (Promega GmbH).

To confirm the CIB1 insertion site in the *Crvt2-1* strain, PCR assays were conducted using gene specific primers that anneal upstream and downstream of the predicted insertion site of the cassette as well as primers specific for the 5' and 3' end of the CIB cassette. Primers 1 (5′-TGATGGCCAAGGGCTTAGTG-3′) and 2 (5'-CCGCAAACACCATGCAATCT-3′) amplified the region of the gene upstream the predicted site of CIB1 cassette insertion (control amplicon with an expected size of 852 bp), primers 3 (5′-AGATTGCATGGTGTTTGCGG-3′) and 4 (5′-CAGGCCATGTGAGAGTTTGCC-3′) amplified the 3' junction site of the CIB1 cassette (amplicon with an expected size of 470 bp), and primers 5 (5′-GCACCAATCATGTCAAGCCT-3′) and 6 (5′-TGTTGTAGCCCACGCGGAAG-3′) amplified the 5' junction site of the cassette (amplicon with an expected size of 601 bp). The primers 11 (5′-GCTCTTGACTCGTTGTGCATTCTAG-3′) and 12 (5'-CACTGAGACACGTCGTACCTG -3′) amplified the 3' junction site of the *PsaD* promoter with the *VTC2* gene in the plasmid used for complementation (amplicon with an expected size of 841 bp).

Analyses of gene expression

Sample collection and RNA isolation was performed as in Vidal-Meireles et al., (2017). The primer pairs for the *VTC2* gene and the reference genes (*bTub2* - Cre12.g549550, *actin* - Cre13.g603700, *UBQ* - XP_001694320) used in RT-qPCR were published earlier in Vidal-

513 Meireles et al. (2017). The annealing sites of the primers for analyzing *VTC2* expression are
514 indicated as primers 7 and 8 in Fig. 1. RT-PCR products using primers 9 (5′-
515 AACCACCTGCACTTCCACGCTTAC-3′) and 10 (5'-TGCCCCGCAATCTCAAACGATG-
516 3′) spanned the sequence encoding the catalytic site of *VTC2* (amplicon with an expected size
517 of 434 bp) were analysed by electrophoresis.

518 The RT-qPCR data are presented as fold-change in mRNA transcript abundance of
519 *VTC2* normalized to the average of the three reference genes and relative to the untreated CC-
520 4533 strain. RT-qPCR analysis was carried out with three technical replicates for each sample
521 and three biological replicates were measured; the standard error was calculated based on the
522 range of fold-change by calculating the minimum and the maximum of the fold-change using
523 the standard deviations of ΔΔCt.

524

525 *Determination of cell size, cell density, chlorophyll, Asc and carotenoid contents*

526 The cell density was determined by a Scepter^{TM} 2.0 hand-held cell counter (Millipore), as
527 described in Vidal-Meireles et al., (2017). Chl content was determined according to Porra
528 (1989), and the Asc content was determined as in Kovács et al., (2016). For carotenoid
529 content determination, liquid culture containing 30 µg Chl(a+b)/ml was filtered onto a
530 Whatman glass microfibre filter (GF/C) and frozen in liquid N_2 at different time points in the
531 NPQ induction protocol. The pigments were extracted by re-suspending the cells in 500 µl of
532 ice-cold acetone. After re-suspension, the samples were incubated in the dark for 30 min.
533 This was followed by centrifugation at 11500 g, 4ºC, for 10 min, and the supernatant was
534 collected and passed through a PTFE 0.2 µm pore size syringe filter.

535 Quantification of carotenoids was performed by HPLC using a Shimadzu Prominence
536 HPLC system (Shimadzu, Kyoto, Japan) consisting of two LC-20AD pumps, a DGU-20A
537 degasser, a SIL-20AC automatic sample injector, CTO-20AC column thermostat and a

Nexera X2 SPD-M30A photodiode-array detector. Chromatographic separations were carried out on a Phenomenex Synergi Hydro-RP 250 x 4.6 mm column with a particle size of 4 µm and a pore size of 80 Å. Twenty-µl aliquots of acetonic extract was injected to the column and the pigments were eluted by a linear gradient from solvent A (acetonitrile, water, triethylamine, in a ratio of 9:1:0.01) to solvent B (ethylacetate). The gradient from solvent A to solvent B was run from 0 to 25 min at a flow rate of 1 ml/min. The column temperature was set to 25 °C. Eluates were monitored in a wavelength range of 260 nm to 750 nm at a sampling frequency of 1.5625 Hz. Pigments were identified according to their retention time and absorption spectrum and quantified by integrated chromatographic peak area recorded at the wavelength of maximum absorbance for each kind of pigments using the corresponding molar decadic absorption coefficient (Jeffrey et al., 1997). The de-epoxidation index of the xanthophyll cycle components was calculated as (zeaxanthin + antheraxanthim)/(violaxanthin + anteraxanthin + zeaxanthin).

Chemical treatments

For Asc supplementation, 1 mM Na-Asc (Roth GmbH) was added to the cultures, and measurements were carried out after a 2 h incubation period in the light. For H_2O_2 treatments, the cell density was adjusted to 3 million cells/ml, and 1.5 mM H_2O_2 (Sigma Aldrich) was added. The presented measurements were carried out 7 h following the addition of H_2O_2. Catalase (5 µg/ml, from bovine liver, Sigma Aldrich) was added after a 30-min dark adaptation, and the measurements were carried out after an additional 2 h incubation period in the dark with shaking.

Immunoblot analysis

562 Protein isolation and immunoblot analysis were performed as in Vidal-Meireles et al., (2017).
563 Specific polyclonal antibodies (produced in rabbits) against PsaA, PsbA, RbcL, LHCSR3,
564 CP43, and PetB were purchased from Agrisera AB. Specific polyclonal antibody (produced
565 in rabbits) against PSBO was purchased from AntiProt.
566
567 *NPQ measurements*
568 Chlorophyll *a* fluorescence was measured using a Dual-PAM-100 instrument (Heinz Walz
569 GmbH, Germany). *C. reinhardtii* cultures were dark-adapted for 30 min and then liquid
570 culture containing 30 µg Chl(a+b)/ml was filtered onto Whatman glass microfibre filters
571 (GF/B) that were placed in between two microscopy cover slips with a spacer to allow for gas
572 exchange. For NPQ induction, light adaptation consisted of 30 min illumination at 530 µmol
573 photons m^{-2} s^{-1}, followed by 12 min of dark adaptation interrupted with saturating pulses of
574 3000 µmol photons m^{-2} s^{-1}.
575
576 *Low-temperature fluorescence emission spectra (77K) measurements*
577 Algal cultures containing 2 µg Chl(a+b)/ml were collected at several time points during the
578 NPQ induction protocol. Subsequently, the sample was filtered onto a Whatman glass
579 microfibre filter (GF/C), placed in a sample holder and immediately frozen in liquid N_2. Low-
580 temperature (77K) fluorescence emission spectra were measured using a spectrofluorometer
581 (Fluorolog- 3/Jobin–Yvon–Spex Instrument S.A., Inc.) equipped with a home-made liquid
582 nitrogen cryostat. The fluorescence emission spectra between 650 and 750 nm were recorded
583 with an interval of 0.5 nm, using an excitation wavelength of 436 nm and excitation and
584 emission slits of 5 and 2 nm, respectively. The final spectra were corrected for the
585 photomultiplier's spectral sensitivity.
586

Statistics

The presented data are based on at least three independent experiments. When applicable, averages and standard errors (±SE) were calculated. Statistical significance was determined using one-way ANOVA followed by Dunnett multiple comparison post-tests (GraphPad Prism 7.04; GraphPad Software, USA). Changes were considered statistically significant at $p < 0.05$.

Accession Numbers

The accession numbers for *C. reinhardtii* genes *VTC2*, *NPQ1* and *STT7* are Cre13.g588150, Cre09.g388060, and Cre02.g120250, respectively. The *Crvtc2-1* mutant strain from the CLiP library is LMJ.RY0402.058624.

Supplemental Data Titles

Supplemental Figure S1. Confirmation of the location of the CIB1 casette in the insertional CLiP mutant of *C. reinhardtii* affected in the *VTC2* gene.

Supplemental Figure S2. Characterization of the CC-4533, *Crvtc2-1* mutant, and *Crvtc2-1+VTC2* complemented *C. reinhardtii* lines in terms of cell volume, Chl content, culture growth and Asc contents.

Supplemental Figure S3. Immunoblot analysis for the semi-quantitative determination of PsbA, CP43, PSBO, PsaA, LHCSR3, PetB and RbcL contents in *Crvtc2-1* and *npq1 C. reinhardtii* mutants.

Supplemental Figure S4. NPQ kinetics induced by strong red light in the *Crvtc2-1* mutant, *Crvtc2-1+VTC2* complemented lines and in a *VTC2-amiRNA* line grown either in photomixotrophic conditions in TAP medium.

Supplemental Figure S5. Carotenoid contents of the *Crvtc2-1* mutant and the wild type during NPQ induction by strong red light.

Supplemental Figure S6. NPQ induction in the *stt7-9* mutant of *C. reinhardtii* and in *cw15-412*.

Supplemental Figure S7. Carotenoid contents of the *Crvtc2-1* mutant and the wild type during NPQ induction upon strong red light.

Supplemental Figure S8. Acclimation to 530 µmol photons m^{-2} s^{-1} of red light followed by recovery in CC-4533 and *Crvtc2-1* cultures grown photoautotrophically in HS medium at 100 µmol photons m^{-2} s^{-1}.

Supplemental Data Legends

Supplemental Figure S1. Confirmation of the location of the CIB1 casette in the insertional CLiP mutant of *C. reinhardtii* (LMJ.RY0402.058624, named *Crvtc2-1*) affected in the *VTC2* gene.

Supplemental Figure S2. Characterization of the CC-4533 (wild-type), *Crvtc2-1* mutant, and *Crvtc2-1+VTC2* complemented *C. reinhardtii* lines in terms of cell volume, Chl content, culture growth and Asc contents.

Supplemental Figure S3. Immunoblot analysis for the semi-quantitative determination of PsbA, CP43, PSBO, PsaA, LHCSR3, PetB and RbcL contents in *Crvtc2-1* and *npq1 C. reinhardtii* mutants.

Supplemental Figure S4. NPQ kinetics induced by strong red light (530 µmol photons m^{-2} s^{-1}) in the *Crvtc2-1* mutant, *Crvtc2-1+VTC2* complemented lines and in a *VTC2-amiRNA* line grown either in photomixotrophic conditions in TAP medium at 100 µmol photons m^{-2} s^{-1} or in photoautotrophic conditions in HS medium at 530 µmol photons m^{-2} s^{-1}.

Supplemental Figure S5. Carotenoid contents of the *Crvtc2-1* mutant and the wild type (CC-4533) during NPQ induction by strong red light (530 µmol photons m^{-2} s^{-1}). The cultures were grown in photomixotrophic conditions in TAP medium at 100 µmole photons m^{-2} s^{-1}.

Supplemental Figure S6. NPQ induction in the *stt7-9* mutant of *C. reinhardtii* and in *cw15-412*, used as a control strain, grown in TAP medium at 100 µmol photons m^{-2} s^{-1}.

Supplemental Figure S7. Carotenoid contents of the *Crvtc2-1* mutant and the wild type (CC-4533) during NPQ induction upon strong red light (530 µmol photons m^{-2} s^{-1}). The cultures were grown in photoautotrophic conditions in HS medium at 530 µmole photons m^{-2} s^{-1}.

Supplemental Figure S8. Acclimation to 530 µmol photons m^{-2} s^{-1} of red light followed by recovery in CC-4533 and *Crvtc2-1* cultures grown photoautotrophically in HS medium at 100 µmol photons m^{-2} s^{-1}.

Acknowledgements:

The authors thank Prof. Dr. Ralph Bock (MPI-MP Potsdam, Germany) and Dr. Petar Lambrev (BRC Szeged, Hungary) for discussions, Dr. Anikó Galambos (BRC Szeged, Hungary) for the assistance with ordering the mutants from the CLiP library, and for Dr. László Szabados (BRC Szeged, Hungary) for the use of their CCD camera.

No conflicts of interest declared.

Figure legends

Figure 1. Characterization of an insertional CLiP mutant of *C. reinhardtii* (LMJ.RY0402.058624, named *Crvtc2-1* mutant) affected in the *VTC2* gene that encodes GDP-L-galactose phosphorylase. A, Physical map of *VTC2* (obtained from Phytozome v12.1.6) with the CIB1 cassette insertion site in the *Crvtc2-1* mutant. Exons are shown in black, introns in light grey, and promoter/ 5' UTR and terminator sequences in dark grey. Insertion site of the CIB1 cassette is indicated by the triangle and the binding sites of the primers used for genotyping and gene expression analysis of *Crvtc2-1* are shown as black arrows. The sequence encoding the catalytic site of GDP-L-galactose phosphorylase is marked as a white line within Exon 3; B, PCR performed using primers annealing upstream the predicted cassette insertion site in *VTC2* (top panel, using primers P1+P2), and using primers amplifying the 5' and 3' genome-cassette junctions (using primers P3+P4 and P5+P6, respectively, middle and bottom panels). The expected sizes are marked with arrows; C, Ascorbate contents of the wild type (CC-4533) and the *Crvtc2-1* mutant grown mixotrophically in TAP medium at moderate light with and without the addition of 1.5 mM H_2O_2; D, Transcript levels of *VTC2*, as determined by RT-qPCR in cultures supplemented or not with H_2O_2 using primers P7+P8. E, Electrophoresis of RT-PCR products using primers P9+P10, spanning the sequence that encodes the catalytic site of GDP-L-galactose phosphorylase. The number of PCR cycles is indicated at the bottom of the figure. The presented data are based on three independent experiments. When applicable, averages and standard errors (±SE) were calculated. Data were analyzed by one-way ANOVA followed by Dunnett's post-test: × $p<0.05$, ×× $p<0.01$, ×××× $p<0.0001$ compared to the untreated CC-4533 strain.

Figure 2. Complementation of the insertional CLiP mutant LMJ.RY0402.058624 affected in the *VTC2* gene (named *Crvtc2-1* mutant) with the coding sequence of *VTC2*. A, Physical map of the *Crvtc2-1+VTC2* plasmid containing the coding sequence of *VTC2*, the constitutive promoter *PsaD* and the *APH7"* resistance gene. Exons are shown in black and promoter/ 5' UTR terminator sequences in dark grey, and the sequence encoding the catalytic site of GDP-L-galactose phosphorylase is marked as a white line. The binding sites of the primers used below are shown as black arrows; B, PCR performed using primers annealing in the promoter and *VTC2* exon 1 (P11+P12). The expected size is marked with an arrow; C, Electrophoresis of RT-PCR products obtained using primers annealing to the sequence encoding the catalytic site of *VTC2* (P9+P10). The expected size is marked with an arrow; D, Ascorbate contents of CC-4533, the *Crvtc2-1* mutant and the complementation lines *Crvtc2-1+VTC2* grown for 3 days in TAP at 100 µmol photons m^{-2} s^{-1}. The presented data are based on four independent experiments. When applicable, averages and standard errors (±SE) were calculated. Data were analyzed by one-way ANOVA followed by Dunnett's post-test: × $p<0.05$, ××× $p<0.001$, ×××× $p<0.0001$ compared to the CC-4533 strain. µE stands for µmol photons m^{-2} s^{-1}.

Figure 3. Acclimation to 530 µmol photons m^{-2} s^{-1} of red light followed by recovery in CC-4533 (wild type) and *Crvtc2-1* cultures grown photomixotrophically in TAP medium at 100 µmol photons m^{-2} s^{-1}. A, NPQ kinetics; B, De-epoxidation index; C, F_V/F_M parameter measured after dark adaptation and after recovery from the 530 µmol photons m^{-2} s^{-1} red light; D, 684 nm/ 710 nm ratio of the 77K fluorescence spectra. Samples were collected at the growth light of 100 µmol photons m^{-2} s^{-1}, after 30 min of dark-adaptation, at the end of the 30 min light period with 530 µmol photons m^{-2} s^{-1} and 15 min after the cessation of actinic illumination, as indicated by arrows in the scheme in panel A. The presented data are based on five independent experiments. When applicable, averages and standard errors (±SE) were

calculated. Data were analyzed by one-way ANOVA followed by Dunnett's post-test: ## $p<0.01$ compared to the CC-4533 strain at the respective time-point; × $p<0.05$, ×× $p<0.01$, ××× $p<0.001$ compared to the dark-adapted CC-4533 strain. µE stands for µmol photons m^{-2} s^{-1}.

Figure 4. Effects of overnight (16 h) dark acclimation on the CC-4533 and the *Crvtc2-1* (grown in TAP medium at 100 µmol photons m^{-2} s^{-1}). A, Ascorbate content after 16 h of dark acclimation; B, NPQ, induced by 530 µmol photons m^{-2} s^{-1} of red light after overnight dark acclimation; C, De-epoxidation index, determined in the overnight dark-acclimated cultures after strong red-light illumination and following recovery. The presented data are based on four independent experiments. When applicable, averages and standard errors (±SE) were calculated. Data were analyzed by one-way ANOVA followed by Dunnett's post-test: ××× $p<0.001$, ×××× $p<0.0001$ compared to the dark-acclimated CC-4533 strain. µE stands for µmol photons m^{-2} s^{-1}.

Figure 5. The effects of H_2O_2 and catalase on NPQ induced by strong red light (530 µmol photons m^{-2} s^{-1}) in the wild type (CC-4533) and the *Crvtc2-1* mutant grown in photomixotrophic conditions in TAP medium at 100 µmol photons m^{-2} s^{-1}. A, The effect of 1.5 mM H_2O_2 on NPQ induction in the CC-4533 strain; B, the effect of 1.5 mM H_2O_2 on NPQ induction in the *Crvtc2-1* mutant; C, the effect of H_2O_2 addition on de-epoxidation; D, the effect of catalase on NPQ induction in the CC-4533 strain; E, the effect of catalase on NPQ induction in the *Crvtc2-1* mutant. Samples were collected at the time points indicated by arrows in the schemes in panels A and B. The presented data are based on three independent experiments. When applicable, averages and standard errors (±SE) were calculated. Data were analyzed by one-way ANOVA followed by Dunnett's post-test: ##

730 $p<0.01$, ### $p<0.001$, #### $p<0.0001$ compared to the untreated CC-4533 culture at the
731 respective time-point; × $p<0.05$, ×× $p<0.01$, ××× $p<0.001$ compared to the dark-adapted CC-
732 4533 strain. µE stands for µmol photons m^{-2} s^{-1}.
733
734 **Figure 6.** Effects of strong red light (530 µmol photons m^{-2} s^{-1}) on the 137a (wild type) and
735 the *npq1* mutant of *C. reinhardtii* grown in TAP medium at 100 µmol photons m^{-2} s^{-1}. A,
736 NPQ induced by 530 µmol photons m^{-2} s^{-1} of red light followed by a recovery phase; B,
737 F_V/F_M values determined before the strong red light illumination and after the recovery phase;
738 C, Chl(a+b) content of the cultures determined before, during and after the strong red light
739 illumination; D, β-carotene content measured before, during and after the strong red light
740 illumination; E, 684 nm/ 710 nm ratio of the 77K fluorescence spectra determined before,
741 during and after the strong red light illumination; F, Ascorbate contents of the *npq1* and
742 *Crvtc2-1* mutants and the CC-4533 and 137a wild-type strains. Samples were collected at the
743 time points indicated by arrows in the scheme in panel A. The presented data are based on
744 five independent experiments. When applicable, averages and standard errors (±SE) were
745 calculated. Data were analyzed by one-way ANOVA followed by Dunnett's post-test: ####
746 $p<0.0001$ compared to the 137a strain at the respective time-point; + $p<0.05$, ++ $p<0.01$,
747 ++++ $p<0.0001$ compared to the dark-adapted 137a strain; ×× $p<0.01$, ×××× $p<0.0001$
748 compared to the CC-4533 strain. µE stands for µmol photons m^{-2} s^{-1}.
749
750 **Figure 7.** Acclimation to 530 µmol photons m^{-2} s^{-1} of red light followed by recovery in CC-
751 4533 and *Crvtc2-1* cultures grown photoautotrophically in HS medium at 530 µmol photons
752 m^{-2} s^{-1}. A, NPQ kinetics; B, De-epoxidation index; C, F_V/F_M parameter measured after dark
753 adaptation and after recovery from the 530 µmol photons m^{-2} s^{-1} red light illumination; D,
754 684 nm/ 710 nm ratio of the 77K fluorescence spectra. The samples were collected at the

growth light of 530 µmol photons m^{-2} s^{-1}, after 30 min of dark adaptation, at the end of the 30 min red light illumination, and 12 min after the cessation of actinic illumination, as indicated in the scheme in panel A. The presented data are based on eight independent experiments. When applicable, averages and standard errors (±SE) were calculated. Data were analyzed by one-way ANOVA followed by Dunnett's post-test: #### $p<0.0001$ compared to the CC-4533 strain at the respective time-point; × $p<0.05$, ×× $p<0.01$, ××× $p<0.001$ compared to the dark-adapted CC-4533 strain. µE stands for µmol photons m^{-2} s^{-1}.

Figure 8. The effects of H_2O_2 and catalase on NPQ induced by strong red light (530 µmol photons m^{-2} s^{-1}) in the wild-type (CC-4533) and *Crvtc2-1* mutant strains grown photoautotrophically in HS medium at 530 µmol photons m^{-2} s^{-1}. A, The effect of 1.5 mM H_2O_2 on NPQ induction in the CC-4533 strain; B, the effect of 1.5 mM H_2O_2 on NPQ induction in the *Crvtc2-1* mutant; C, the effect of catalase on NPQ induction in the CC-4533 strain; D, the effect of catalase on NPQ induction in the *Crvtc2-1* mutant. The presented data are based on four independent experiments. When applicable, averages and standard errors (±SE) were calculated. Data were analyzed by one-way ANOVA followed by Dunnett's post-test: # $p<0.05$, #### $p<0.0001$ compared to the untreated CC-4533 culture at the respective time-point. µE stands for µmol photons m^{-2} s^{-1}.

773 **Literature Cited**

774

775 Adams WW III, Muller O, Cohu CM, Demmig-Adams B (2013) May photoinhibition be a
776 consequence, rather than a cause, of limited plant productivity? Photosynth Res 117:31-
777 44

778 Allorent G, Tokutsu R, Roach T, Peers G, Cardol P, Girard-Bascou J, Seigneurin-Berny D,
779 Petroutsos D, Kuntz M, Breyton C, Franck F, Wollman FA, Niyogi KK, Krieger-
780 Liszkay A, Minagawa J, Finazzi G (2013) A dual strategy to cope with high light in
781 *Chlamydomonas reinhardtii*. Plant Cell 25:545-557

782 Anwaruzzaman M, Chin BL, Li X-P, Lohr M, Martinez DA, Niyogi KK (2004) Genomic
783 analysis of mutants affecting xanthophyll biosynthesis and regulation of photosynthetic
784 light harvesting in Chlamydomonas reinhardtii. Photosynth Res 82:265-276

785 Arnoux P, Morosinotto T, Saga G, Bassi R, Pignol D (2009) A structural basis for the pH-
786 dependent xanthophyll cycle in *Arabidopsis thaliana*. Plant Cell 21: 2036-2044

787 Asada K (2006) Production and scavenging of reactive oxygen species in chloroplasts and
788 their functions. Plant Physiol 141: 391-396

789 Avenson TJ, Ahn TK, Zigmantas D, Niyogi KK, Li Z, Ballottari M, Bassi R, Fleming GR
790 (2008) Zeaxanthin radical cation formation in minor light-harvesting complexes of
791 higher plant antenna. J Biol Chem 283:3550-3558

792 Azzabi G, Pinnola A, Betterle N, Bassi R, Alboresi A (2012) Enhancement of non-photo de-
793 epoxidation index chemical quenching in the bryophyte *Physcomitrella patens* during
794 acclimation to salt and osmotic stress. Plant Cell Physiol 53: 1815-1825

795 Barahimipour R, Strenkert D, Neupert J, Schroda M, Merchant SS, Bock R (2015) Dissecting
796 the contributions of GC content and codon usage to gene expression in the model alga
797 *Chlamydomonas reinhardtii*. Plant J 84: 704-717

798 Baroli I, Do AD, Yamane T, Niyogi KK (2003) Zeaxanthin accumulation in the absence of a
799 functional xanthophyll cycle protects *Chlamydomonas reinhardtii* from photooxidative
800 stress. Plant Cell 15: 992-1008
801 Bratt C, Arvidsson P, Carlsson M, Akerlund H (1995) Regulation of violaxanthin de-
802 epoxidase activity by pH and ascorbate. Photosynth Res 45: 169-175
803 Bonente G, Ballottari M, Truong T, Morosinotto T, Ahn T, Fleming G, Niyogi K, Bassi R
804 (2011) Analysis of LhcSR3, a protein essential for feedback de- excitation in the green
805 alga *Chlamydomonas reinhardtii*. PLoS Biol 9:e1000577
806 Bradbury LMT, Shumskaya M, Tzfadia O, Wu S-B, Kennelly EK, Wurtzelt ET (2012)
807 Lycopene cyclase paralog CruP protects against reactive oxygen species in oxygenic
808 photosynthetic organisms. Proc Natl Acad Sci USA 109:E1888-E1897
809 Chaux F, Johnson X, Auroy P, Beyly-Adriano A, Te I, Cuiné S, Peltier G (2017) PGRL1 and
810 LHCSR3 compensate for each other in controlling photosynthesis and avoiding
811 photosystem I photoinhibition during high light acclimation of Chlamydomonas cells.
812 Mol Plant 10:216-218
813 Christa G, Cruz S, Jahns P, de Vries J, Cartaxana P, Esteves AC, Serôdio J, Gould SB (2017)
814 Photoprotection in a monophyletic branch of chlorophyte algae is independent of
815 energy-dependent quenching (qE). New Phytol 214: 1132-1144
816 Depège N, Bellafiore S, Rochaix JD (2003) Role of chloroplast protein kinase Stt7 in LHCII
817 phosphorylation and state transition in Chlamydomonas. Science 299: 1572-1575
818 Dowdle J, Ishikawa T, Gatzek S, Rolinski S, Smirnoff N (2007) Two genes in *Arabidopsis*
819 *thaliana* encoding GDP-L-galactose phosphorylase are required for ascorbate
820 biosynthesis and seedling viability. Plant J 52: 673-689
821 Erickson E, Wakao S, Niyogi KK (2015) Light stress and photoprotection in *Chlamydomonas*
822 *reinhardtii.* Plant J 82:449-465

823 Fernie AR, Tóth SZ (2015) Identification of the elusive chloroplast ascorbate transporter
824 extends the substrate specificity of the PHT family. Mol Plant 8:674-676
825 Finazzi G, Johnson GN, Dall'Osto L, Zito F, Bonente G, Bassi R, Wollman F-A (2006)
826 Nonphotochemical quenching of chlorophyll fluorescence in *Chlamydomonas*
827 *reinhardtii*. Biochemistry 45:1490-1498
828 Foyer CH, Shigeoka S (2011) Understanding oxidative stress and antioxidant functions to
829 enhance photosynthesis. Plant Physiol 155: 93-100
830 Gest N, Gautier H, Stevens R (2013) Ascorbate as seen through plant evolution: the rise of a
831 successful molecule? J Exp Bot 64:33-53
832 Grouneva I, Jakob T, Wilhelm C, Goss R (2006) Influence of ascorbate and pH on the
833 activity of the diatom xanthophyll cycle-enzyme diadinoxanthin de-epoxidase. Physiol
834 Plant 126:205-211
835 Hager A, Holocher K (1994) Localization of the xanthophyll-cycle enzyme violaxanthin de-
836 epoxidase within the thylakoid lumen and abolition of its mobility by a (light-
837 dependent) pH decrease. Planta 192: 581-589
838 Hallin EI, Hasan M, Guo K, Åkerlund H-E (2016) Molecular studies on structural changes
839 and oligomerisation of violaxanthin de-epoxidase associated with the pH-dependent
840 activation. Photosynth Res 129: 29-41
841 Hieber AD, Bugos RC, Yamamoto HY (2000) Plant lipocalins: violaxanthin de-epoxidase
842 and zeaxanthin epoxidase. Biochim Biophys Acta BBA - Protein Struct Mol Enzymol
843 1482: 84-91
844 Holt NE, Zigmantas D, Valkunas L, Li X-P, Niyogi KK, Fleming GR (2005) Carotenoid
845 cation formation and the regulation of photosynthetic light harvesting. Science
846 307:433-436

847 Holub O, Seufferheld MJ, Gohlke C, Heiss GJ, Clegg RM (2007) Fluorescence lifetime
848 imaging microscopy of *Chlamydomonas reinhardtii*: non-photochemical quenching
849 mutants and the effect of photosynthetic inhibitors on the slow chlorophyll fluorescence
850 transient. J Microsc 226: 90-120
851 Ivanov B, Asada K, Edwards GE (2007) Analysis of donors of electrons to photosystem I and
852 cyclic electron flow by redox kinetics of P700 in chloroplasts of isolated bundle sheath
853 strands of maize. Photosynth Res 92:65-74
854 Iwai M, Kato N, Minagawa J (2007) Distinct physiological responses to a high light and low
855 CO_2 environment revealed by fluorescence quenching in photoautotrophically grown
856 *Chlamydomonas reinhardtii*. Photosynth Res 94:307-314
857 Jeffrey SW, Mantoura RFC, Wright SW (1997) Phytoplankton pigments in oceanography:
858 guidelines to modern methods. (Paris: UNESCO Publishing)
859 Johnson X, Alric J (2012) Interaction between starch breakdown, acetate assimilation, and
860 photosynthetic cyclic electron flow in *Chlamydomonas reinhardtii*. J Biol Chem
861 287:26445-26452
862 Johnson MP, Davison PA, Ruban AV, Horton P (2008) The xanthophyll cycle pool size
863 controls the kinetics of non-photochemical quenching in *Arabidopsis thaliana*. FEBS
864 Lett 582:259-263
865 Kanazawa A, Kramer DM (2002). In vivo modulation of nonphotochemical exciton
866 quenching (NPQ) by regulation of the chloroplast ATP synthase. Proc Natl Acad Sci
867 USA 99:12789-12794
868 Kovács L, Vidal-Meireles A, Nagy V, Tóth SZ (2016) Quantitative determination of
869 ascorbate from the green alga *Chlamydomonas reinhardtii* by HPLC. Bio-Protoc
870 6:e2067

871 Lemeille S, Willig A, Depège-Fargeix N, Delessert C, Bassi R, Rochaix J-D (2009) Analysis
872 of the chloroplast protein kinase Stt7 during state transitions. PLoS Biol 7: e1000045
873 Li S, Liu L, Zhuang X, Yu Y, Liu X, Cui X, Ji L, Pan Z, Cao X, Mo B, Zhang F, Raikhel N,
874 Jiang L, and Chen X (2013) MicroRNAs inhibit the Ttranslation of target mRNAs on
875 the endoplasmic reticulum in Arabidopsis. Cell 153: 562-574
876 Li Z, Peers G, Dent RM, Bai Y, Yang SY, Apel W, Leonelli L, Niyogi KK (2016a) Evolution
877 of an atypical de-epoxidase for photoprotection in the green lineage. Nat Plants 2:
878 16140
879 Li X, Zhang R, Patena W, Gang SS, Blum SR, Ivanova N, Yue R, Robertson JM, Lefebvre
880 PA, Fitz-Gibbon ST, Grossman AR, Jonikas MC (2016b) An indexed, mapped mutant
881 library enables reverse genetics studies of biological processes in *Chlamydomonas*
882 *reinhardtii*. Plant Cell 28: 367-387
883 Marschall M, Proctor MCF (2004) Are bryophytes shade plants? Photosynthetic light
884 responses and proportions of chlorophyll *a*, chlorophyll b and total carotenoids. Ann
885 Bot 94: 593-603
886 Müller-Moulé P, Conklin PL, Niyogi KK (2002) Ascorbate deficiency can limit violaxanthin
887 de-epoxidase activity in vivo. Plant Physiol 128: 970-977
888 Müller-Moulé P, Havaux M, Niyogi KK (2003) Zeaxanthin deficiency enhances the high
889 light sensitivity of an ascorbate-deficient mutant of Arabidopsis. Plant Physiol 133:
890 748-760.
891 Nagy V, Vidal-Meireles A, Podmaniczki A, Szentmihályi K, Rákhely G, Zsigmond L,
892 Kovács L, Tóth SZ (2018) The mechanism of photosystem II inactivation during
893 sulphur deprivation-induced H_2 production in *Chlamydomonas reinhardtii*. Plant J
894 94:548-561

895 Neupert J, Karcher D, Bock R (2009) Generation of Chlamydomonas strains that efficiently
896 express nuclear transgenes. Plant J 57:1140-1150
897 Niyogi KK, Bjorkman O, Grossmann AR (1997) Chlamydomonas xanthophyll cycle mutants
898 identified by video imaging of chlorophyll fluorescence quenching. Plant Cell 9:1369-
899 1380
900 Peers G, Truong TB, Ostendorf E, Busch A, Elrad D, Grossman AR, Hippler M, Niyogi KK
901 (2009) An ancient light-harvesting protein is critical for the regulation of algal
902 photosynthesis. Nature 462:518-521
903 Pinnola A, Dall'Osto L, Gerotto C, Morosinotto T, Bassi R, Alboresi A (2013) Zeaxanthin
904 binds to Light-Harvesting Complex Stress-Related Protein to enhance
905 nonphotochemical quenching in *Physcomitrella patens*. Plant Cell 25:3519-3534
906 Polukhina I, Fristedt R, Dinc E, Cardol P, Croce R (2016) Carbon supply and
907 photoacclimation cross talk in the green alga *Chlamydomonas reinhardtii*. Plant Physiol
908 172: 1494-1505
909 Porra RJ, Thompson WA, Kriedeman PE (1989) Determination of accurate extinction
910 coefficients and simultaneous equations for essaying chlorophylls-a and -b with four
911 different solvents: verification of the concentration of chlorophyll standards by atomic
912 absorption spectroscopy. Biochim Biophys Acta 975: 384-394
913 Quaas T, Berteotti S, Ballottari M, Flieger K, Bassi R, Wilhelm C, Goss R (2015) Non-
914 photochemical quenching and xanthophyll cycle activities in six green algal species
915 suggest mechanistic differences in the process of excess energy dissipation. J. Plant
916 Physiol 172: 92-103
917 Roach T, Na CS (2017) LHCSR3 affects de-coupling and re-coupling of LHCII to PSII
918 during state transitions in *Chlamydomonas reinhardtii*. Sci Rep 7: 43145

Ruban AV, Johnson MP, Duffy CD (2012) The photoprotective molecular switch in the photosystem II antenna. Biochim Biophys Acta 1817:167-181

Saga G, Giorgetti A, Fufezan C, Giacometti GM, Bassi R, Morosinotto T (2010) Mutation analysis of violaxanthin de-epoxidase identifies substrate-binding sites and residues involved in catalysis. J Biol Chem 285:23763-23770

Schroda M, Vallon O, Whitelegge JP, Beck CF, Wollman FA (2001) The chloroplastic GrpE homolog of Chlamydomonas: two isoforms generated by differential splicing. Plant Cell 13:2823-2839

Smirnoff N (2018) Ascorbic acid metabolism and functions: A comparison of plants and mammals. Free Radic Biol Med. 122:116-129

Takizawa K, Kanazawa A, Kramer DM (2008) Depletion of stromal Pi induces high 'energy dependent' antenna exciton quenching (qE) by decreasing proton conductivity at CFO-CF1 ATP synthase. Plant Cell Environ 31:235-243

Tibiletti T, Auroy P, Peltier G, Caffarri S (2016) *Chlamydomonas reinhardtii* PsbS protein is functional and accumulates rapidly and transiently under high light. Plant Physiol 171:2717-2730

Tikkanen M, Mekala NR, Aro E-M (2014) Photosystem II photoinhibition-repair cycle protects photosystem I from irreversible damage. Biochim Biophys Acta - Bioenerg 1837: 210-215

Tóth SZ, Puthur JT, Nagy V, Garab G (2009) Experimental evidence for ascorbate-dependent electron transport in leaves with inactive oxygen-evolving complexes. Plant Physiol 149: 1568-1578

Tóth SZ, Nagy V, Puthur JT, Kovács L, Garab G (2011) The physiological role of ascorbate as photosystem II electron donor: Protection against photoinactivation in heat-stressed leaves. Plant Physiol 156: 382-392

944 Tóth SZ, Lőrincz T, Szarka A (2018) Concentration does matter: The beneficial and
945 potentially harmful effects of ascorbate in humans and plants. Antioxid Redox Signal
946 29:1516-1533
947 Ünlü C, Drop B, Croce R, van Amerongen H (2014) State transitions in *Chlamydomonas*
948 *reinhardtii* strongly modulate the functional size of photosystem II but not of
949 photosystem I. Proc Natl Acad Sci USA 111:3460-3465
950 Urzica EI, Adler LN, Page MD, Linster CL, Arbing MA, Casero D, Pellegrini M, Merchant
951 SS, Clarke SG (2012) Impact of oxidative stress on ascorbate biosynthesis in
952 Chlamydomonas via regulation of the *VTC2* gene encoding a GDP-L-galactose
953 phosphorylase. J Biol Chem 287: 14234-14245
954 Vidal-Meireles A, Neupert J, Zsigmond L, Rosado-Souza L, Kovács L, Nagy V, Galambos
955 A, Fernie AR, Bock R, Tóth SZ (2017) Regulation of ascorbate biosynthesis in green
956 algae has evolved to enable rapid stress-induced response via the *VTC2* gene encoding
957 GDP- L -galactose phosphorylase. New Phytol 214: 668-681
958 Voigt J, Münzner P (1994) Blue light-induced lethality of a cell wall-deficient mutant of the
959 unicellular green alga *Chlamydomonas reinhardtii*. Plant Cell Physiol 35: 99-106
960 Wang Z, Xiao Y, Chen W, Tang K, Zhang L (2010) Increased vitamin C content
961 accompanied by an enhanced recycling pathway confers oxidative stress tolerance in
962 Arabidopsis. J. Integr. Plant Biol 52: 400-409
963 Wheeler G, Ishikawa T, Pornsaksit V, Smirnoff N (2015) Evolution of alternative
964 biosynthetic pathways for vitamin C following plastid acquisition in photosynthetic
965 eukaryotes. eLife 4:e06369
966 Xue H, Tokutsu R, Bergner SV, Scholz M, Minagawa J, Hippler M (2015) Photosystem II
967 subunit R is required for efficient binding of Light-Harvesting Complex Stress-Related

968 Protein 3 to photosystem II-light-harvesting supercomplexes in *Chlamydomonas*
969 *reinhardtii*. Plant Physiol 167: 1566-1578
970 Zechmann B, Stumpe M, Mauch F (2011) Immunocytochemical determination of the
971 subcellular distribution of ascorbate in plants. Planta 233: 1-12

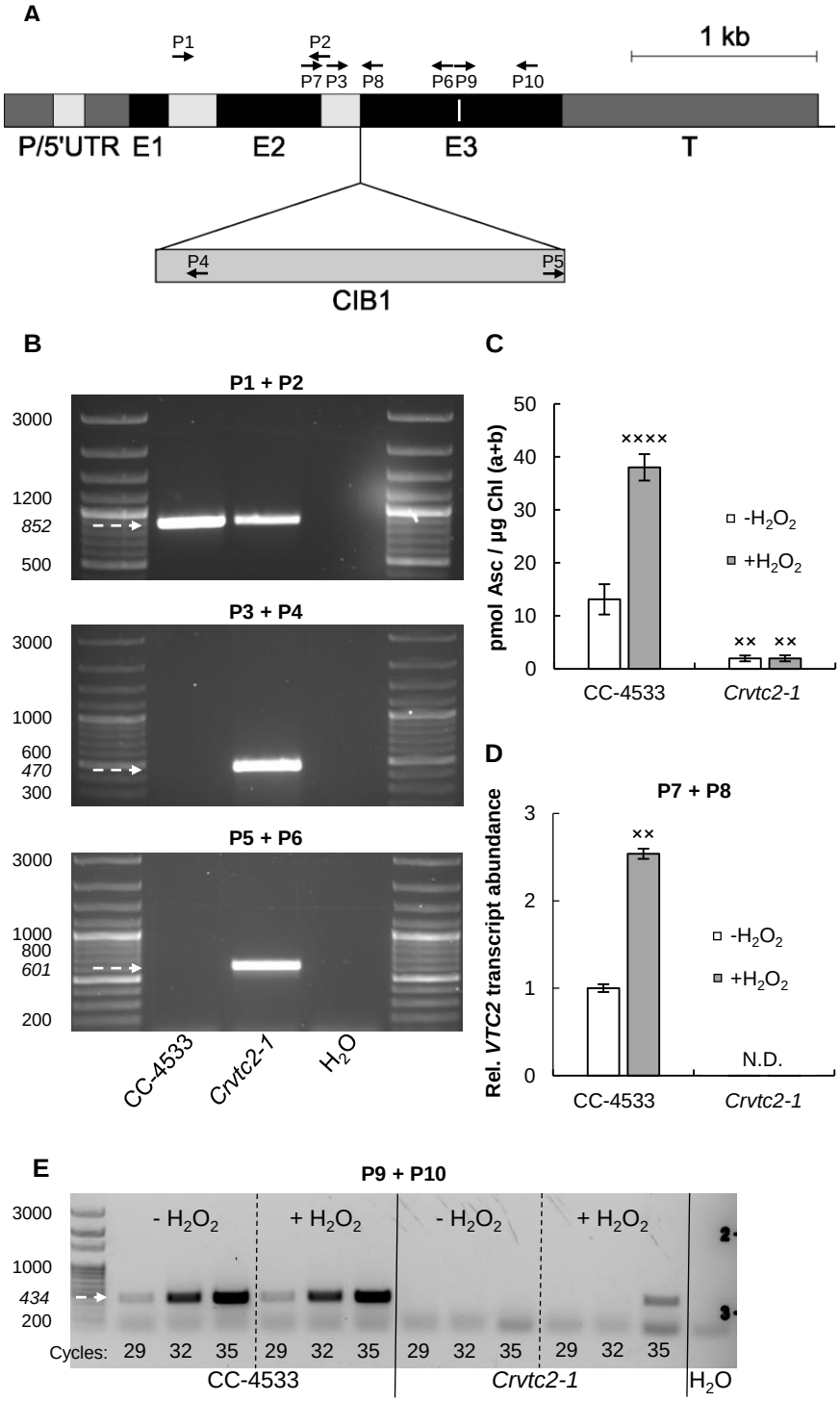

Figure 1. Characterization of an insertional CLiP mutant of *C. reinhardtii* (LMJ.RY0402.058624, named *Crvtc2-1* mutant) affected in the *VTC2* gene that encodes GDP-L-galactose phosphorylase. A, Physical map of *VTC2* (obtained from Phytozome v12.1.6) with the CIB1 cassette insertion site in the *Crvtc2-1* mutant. Exons are shown in black, introns in light grey, and promoter/ 5' UTR and terminator sequences in dark grey. Insertion site of the CIB1 cassette is indicated by the triangle and the binding sites of the primers used for genotyping and gene expression analysis of *Crvtc2-1* are shown as black arrows. The sequence encoding the catalytic site of GDP-L-galactose phosphorylase is marked as a white line within Exon 3; B, PCR performed using primers annealing upstream the predicted cassette insertion site in *VTC2* (top panel, using primers P1+P2), and using primers amplifying the 5' and 3' genome-cassette junctions (using primers P3+P4 and P5+P6, respectively, middle and bottom panels). The expected sizes are marked with arrows; C, Ascorbate contents of the wild type (CC-4533) and the *Crvtc2-1* mutant grown mixotrophically in TAP medium at moderate light with and without the addition of 1.5 mM H_2O_2; D, Transcript levels of *VTC2*, as determined by RT-qPCR in cultures supplemented or not with H_2O_2 using primers P7+P8. E, Electrophoresis of RT-PCR products using primers P9+P10, spanning the sequence that encodes the catalytic site of GDP-L-galactose phosphorylase. The number of PCR cycles is indicated at the bottom of the figure. The presented data are based on three independent experiments. When applicable, averages and standard errors (±SE) were calculated. Data were analyzed by one-way ANOVA followed by Dunnett's post-test: × $p<0.05$, ×× $p<0.01$, ×××× $p<0.0001$ compared to the untreated CC-4533 strain.

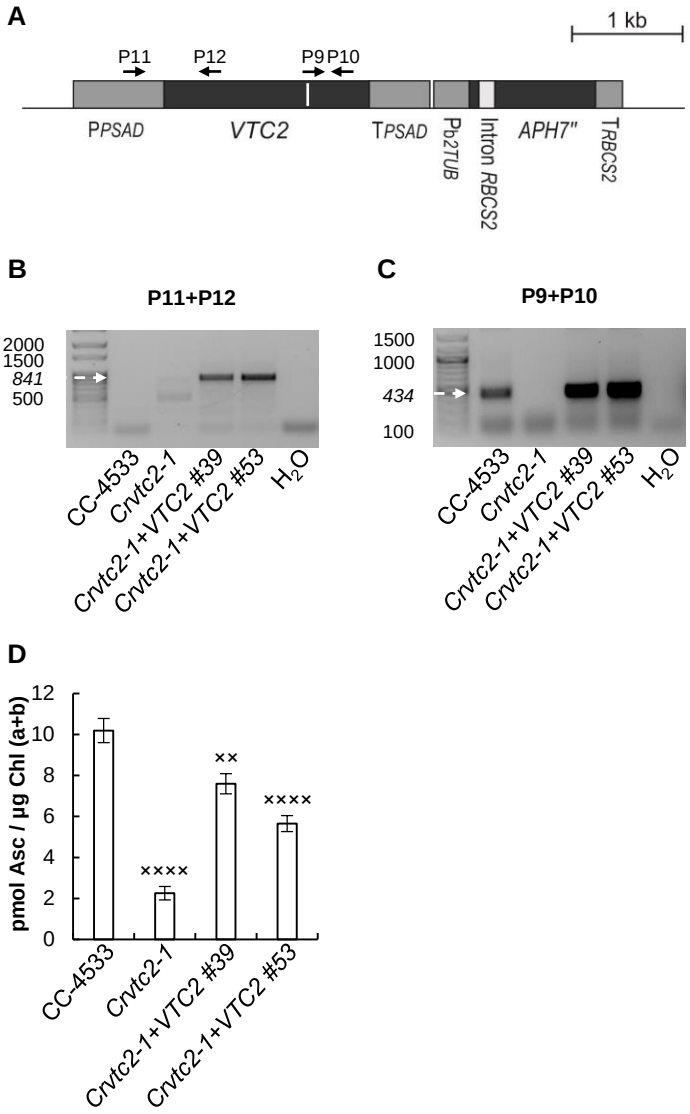

Figure 2 – Complementation of the insertional CLiP mutant LMJ.RY0402.058624 affected in the *VTC2* gene (named *Crvtc2-1* mutant) with the coding sequence of *VTC2*. A, Physical map of the *Crvtc2-1+VTC2* plasmid containing the coding sequence of *VTC2*, the constitutive promoter *PsaD* and the *APH7"* resistance gene. Exons are shown in black and promoter/ 5' UTR terminator sequences in dark grey, and the sequence encoding the catalytic site of GDP-L-galactose phosphorylase is marked as a white line. The binding sites of the primers used below are shown as black arrows; B, PCR performed using primers annealing in the promoter and *VTC2* exon 1 (P11+P12). The expected size is marked with an arrow; C, Electrophoresis of RT-PCR products obtained using primers annealing to the sequence encoding the catalytic site of *VTC2* (P9+P10). The expected size is marked with an arrow; D, Ascorbate contents of CC-4533, the *Crvtc2-1* mutant and the complementation lines *Crvtc2-1+VTC2* grown for 3 days in TAP at 100 µmol photons m^{-2} s^{-1}. The presented data are based on four independent experiments. When applicable, averages and standard errors (±SE) were calculated. Data were analyzed by one-way ANOVA followed by Dunnett's post-test: × p<0.05, ××× p<0.001, ×××× p<0.0001 compared to the CC-4533 strain. µE stands for µmol photons m^{-2} s^{-1}.

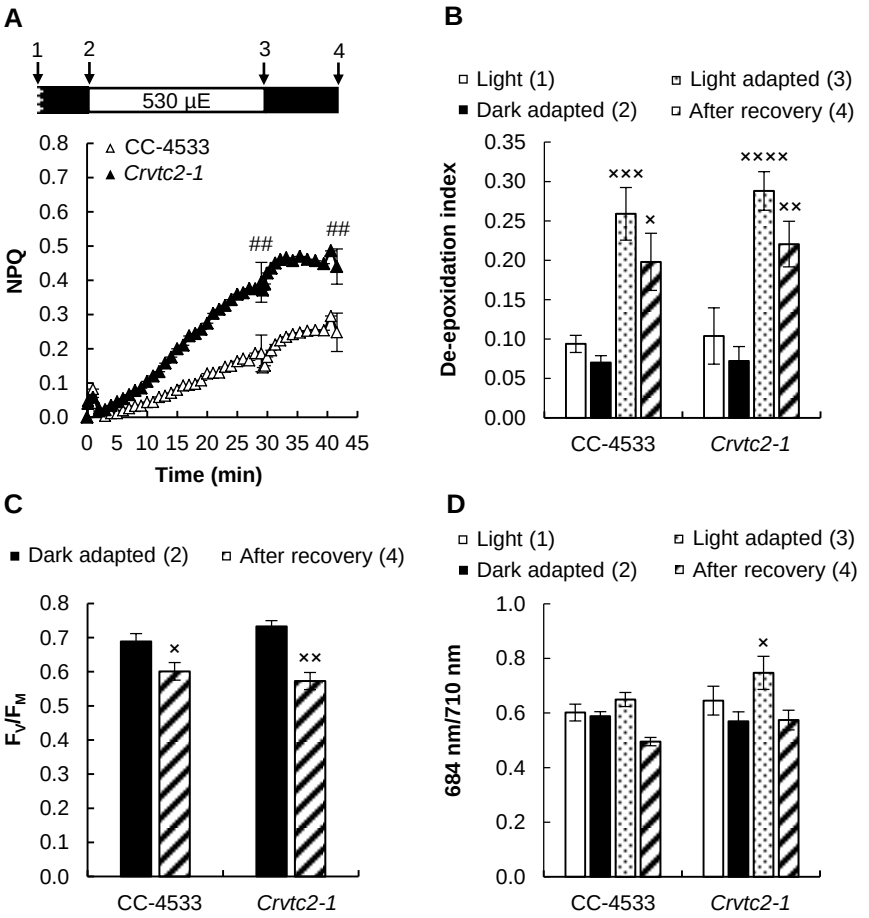

Figure 3 – Acclimation to 530 µmol photons m^{-2} s^{-1} of red light followed by recovery in CC-4533 (wild type) and *Crvtc2-1* cultures grown photomixotrophically in TAP medium at 100 µmol photons m^{-2} s^{-1}. A, NPQ kinetics; B, De-epoxidation index; C, F_V/F_M parameter measured after dark adaptation and after recovery from the 530 µmol photons m^{-2} s^{-1} red light; D, 684 nm/ 710 nm ratio of the 77K fluorescence spectra. Samples were collected at the growth light of 100 µmol photons m^{-2} s^{-1}, after 30 min of dark-adaptation, at the end of the 30 min light period with 530 µmol photons m^{-2} s^{-1} and 15 min after the cessation of actinic illumination, as indicated by arrows in the scheme in panel A. The presented data are based on five independent experiments. When applicable, averages and standard errors (±SE) were calculated. Data were analyzed by one-way ANOVA followed by Dunnett's post-test: ## $p<0.01$ compared to the CC-4533 strain at the respective time-point; × $p<0.05$, ×× $p<0.01$, ××× $p<0.001$ compared to the dark-adapted CC-4533 strain. µE stands for µmol photons m^{-2} s^{-1}.

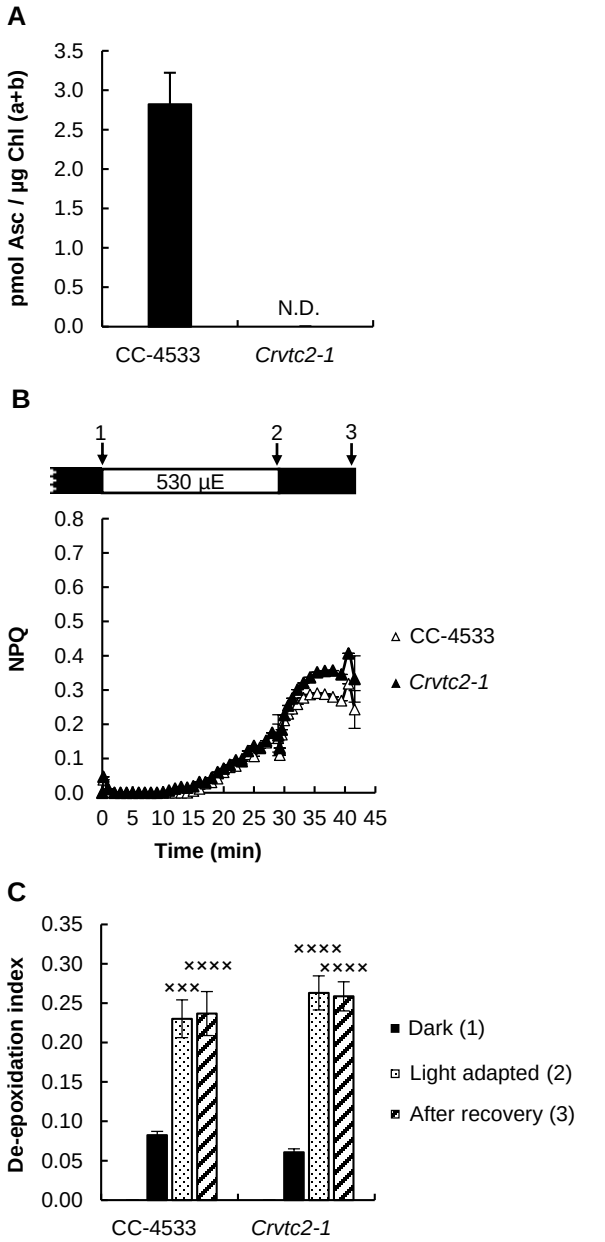

Figure 4 – Effects of overnight (16 h) dark acclimation on the CC-4533 and the *Crvtc2-1* (grown in TAP medium at 100 µmol photons m^{-2} s^{-1}). A, Ascorbate content after 16 h of dark acclimation; B, NPQ, induced by 530 µmol photons m^{-2} s^{-1} of red light after overnight dark acclimation; C, De-epoxidation index, determined in the overnight dark-acclimated cultures after strong red-light illumination and following recovery. The presented data are based on four independent experiments. When applicable, averages and standard errors (±SE) were calculated. Data were analyzed by one-way ANOVA followed by Dunnett's post-test: ××× p<0.001, ×××× p<0.0001 compared to the dark-acclimated CC-4533 strain. µE stands for µmol photons m^{-2} s^{-1}.

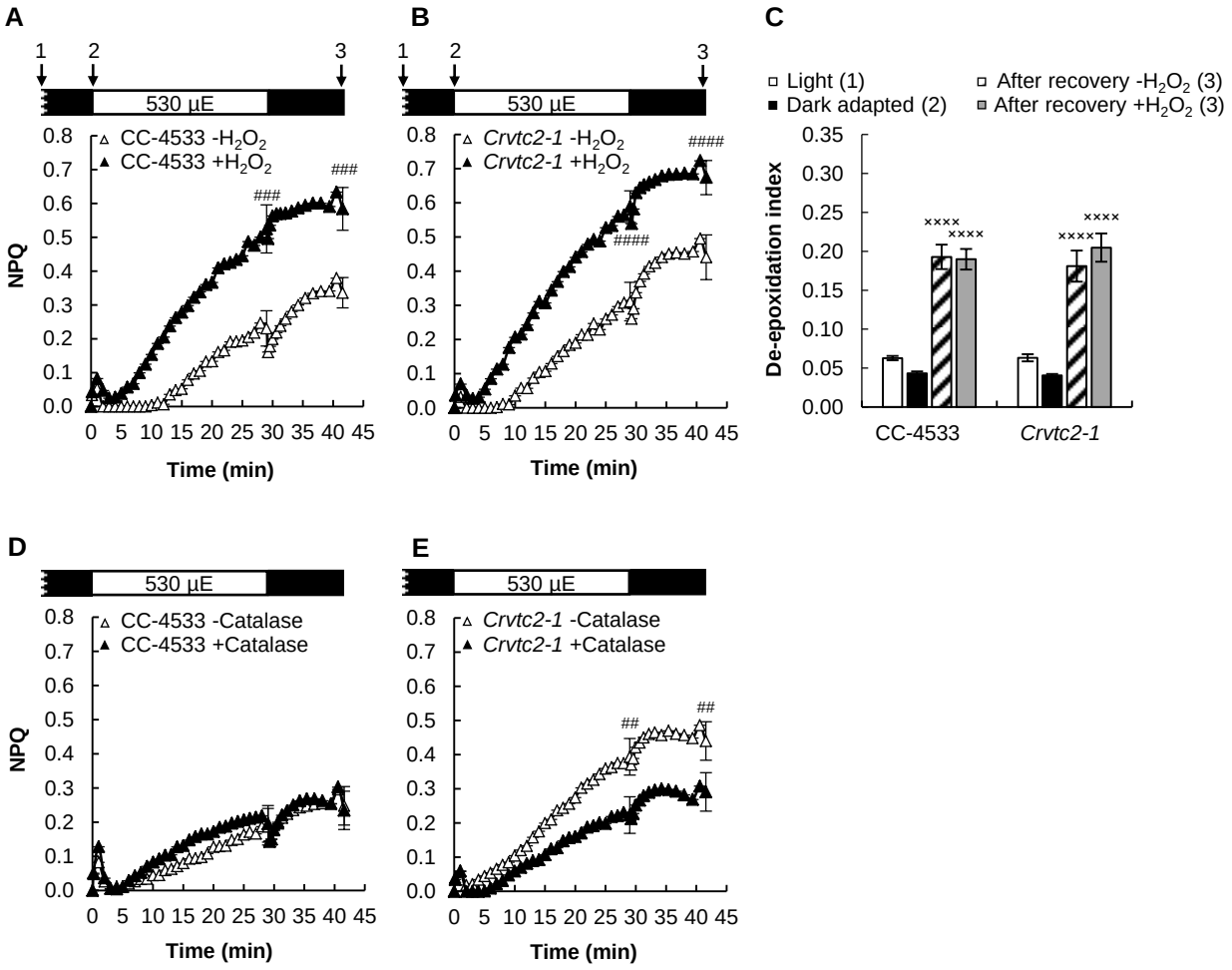

Figure 5 – The effects of H_2O_2 and catalase on NPQ induced by strong red light (530 µmol photons m^{-2} s^{-1}) in the wild type (CC-4533) and the *Crvtc2-1* mutant grown in photomixotrophic conditions in TAP medium at 100 µmol photons m^{-2} s^{-1}. A, The effect of 1.5 mM H_2O_2 on NPQ induction in the CC-4533 strain; B, the effect of 1.5 mM H_2O_2 on NPQ induction in the *Crvtc2-1* mutant; C, the effect of H_2O_2 addition on de-epoxidation; D, the effect of catalase on NPQ induction in the CC-4533 strain; E, the effect of catalase on NPQ induction in the *Crvtc2-1* mutant. Samples were collected at the time points indicated by arrows in the schemes in panels A and B. The presented data are based on three independent experiments. When applicable, averages and standard errors (±SE) were calculated. Data were analyzed by one-way ANOVA followed by Dunnett's post-test: ## p<0.01, ### p<0.001, #### p<0.0001 compared to the untreated CC-4533 culture at the respective time-point; × p<0.05, ×× p<0.01, ××× p<0.001 compared to the dark-adapted CC-4533 strain. µE stands for µmol photons m^{-2} s^{-1}.

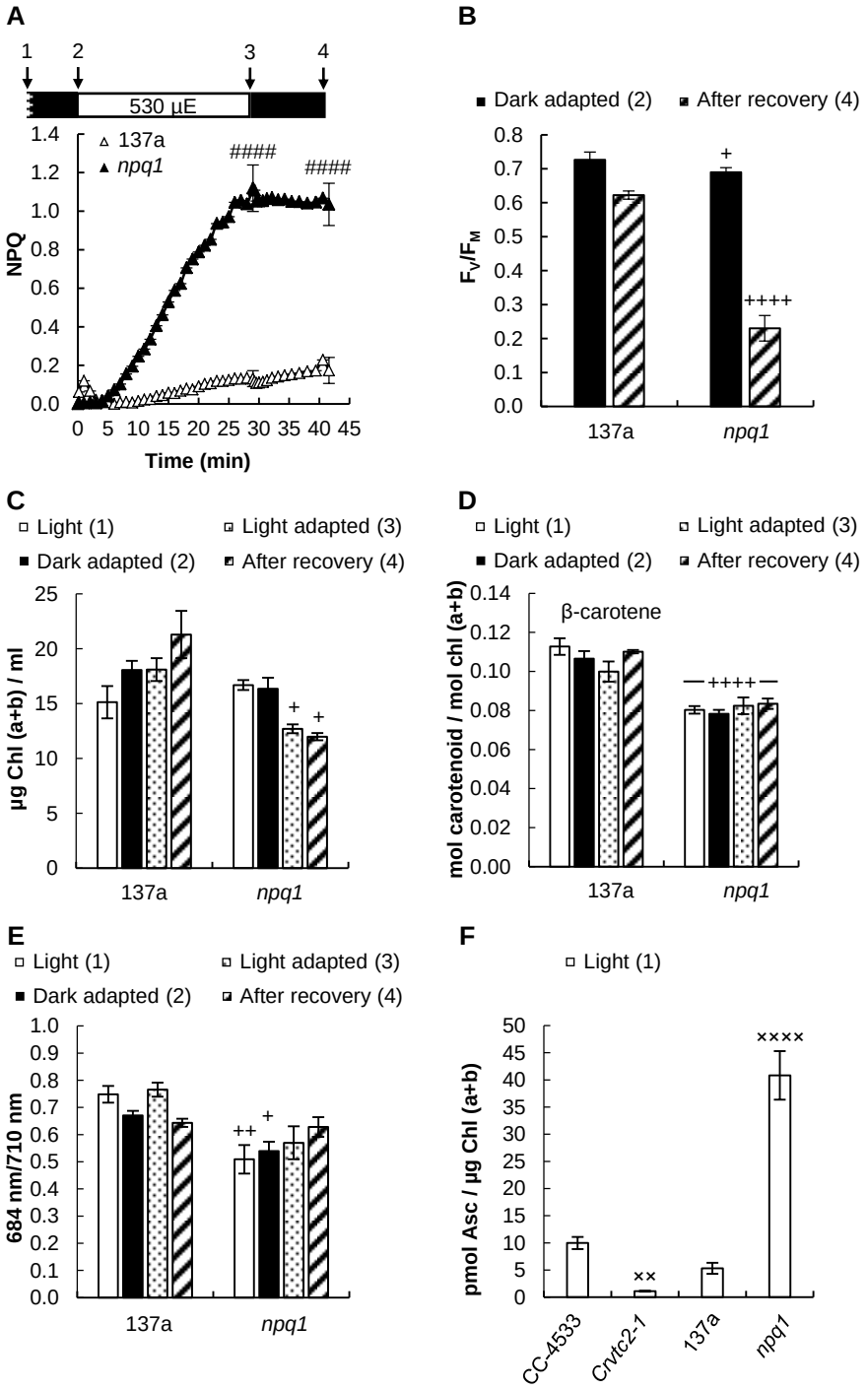

Figure 6 – Effects of strong red light (530 µmol photons m^{-2} s^{-1}) on the 137a (wild type) and the *npq1* mutant of *C. reinhardtii* grown in TAP medium at 100 µmol photons m^{-2} s^{-1}. A, NPQ induced by 530 µmol photons m^{-2} s^{-1} of red light followed by a recovery phase; B, F_V/F_M values determined before the strong red light illumination and after the recovery phase; C, Chl(a+b) content of the cultures determined before, during and after the strong red light illumination; D, β-carotene content measured before, during and after the strong red light illumination; E, 684 nm/ 710 nm ratio of the 77K fluorescence spectra determined before, during and after the strong red light illumination; F, Ascorbate contents of the *npq1* and *Crvtc2-1* mutants and the CC-4533 and 137a wild-type strains. Samples were collected at the time points indicated by arrows in the scheme in panel A. The presented data are based on five independent experiments. When applicable, averages and standard errors (±SE) were calculated. Data were analyzed by one-way ANOVA followed by Dunnett's post-test: #### p<0.0001 compared to the 137a strain at the respective time-point; + p<0.05, ++ p<0.01, ++++ p<0.0001 compared to the dark-adapted 137a strain; ×× p<0.01, ×××× p<0.0001 compared to the CC-4533 strain. µE stands for µmol photons m^{-2} s^{-1}.

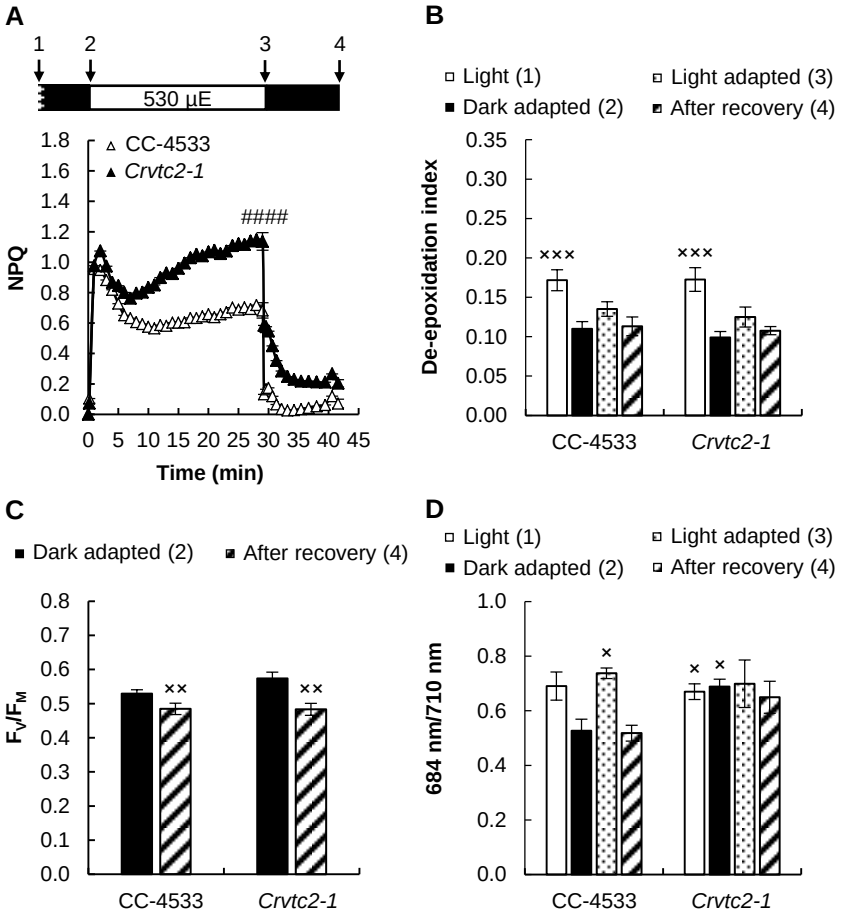

Figure 7 – Acclimation to 530 µmol photons m^{-2} s^{-1} of red light followed by recovery in CC-4533 and *Crvtc2-1* cultures grown photoautotrophically in HS medium at 530 µmol photons m^{-2} s^{-1}. A, NPQ kinetics; B, De-epoxidation index; C, F_V/F_M parameter measured after dark adaptation and after recovery from the 530 µmol photons m^{-2} s^{-1} red light illumination; D, 684 nm/ 710 nm ratio of the 77K fluorescence spectra. The samples were collected at the growth light of 530 µmol photons m^{-2} s^{-1}, after 30 min of dark adaptation, at the end of the 30 min red light illumination, and 12 min after the cessation of actinic illumination, as indicated in the scheme in panel A. The presented data are based on eight independent experiments. When applicable, averages and standard errors (±SE) were calculated. Data were analyzed by one-way ANOVA followed by Dunnett's post-test: #### $p<0.0001$ compared to the CC-4533 strain at the respective time-point; × $p<0.05$, ×× $p<0.01$, ××× $p<0.001$ compared to the dark-adapted CC-4533 strain. µE stands for µmol photons m^{-2} s^{-1}.

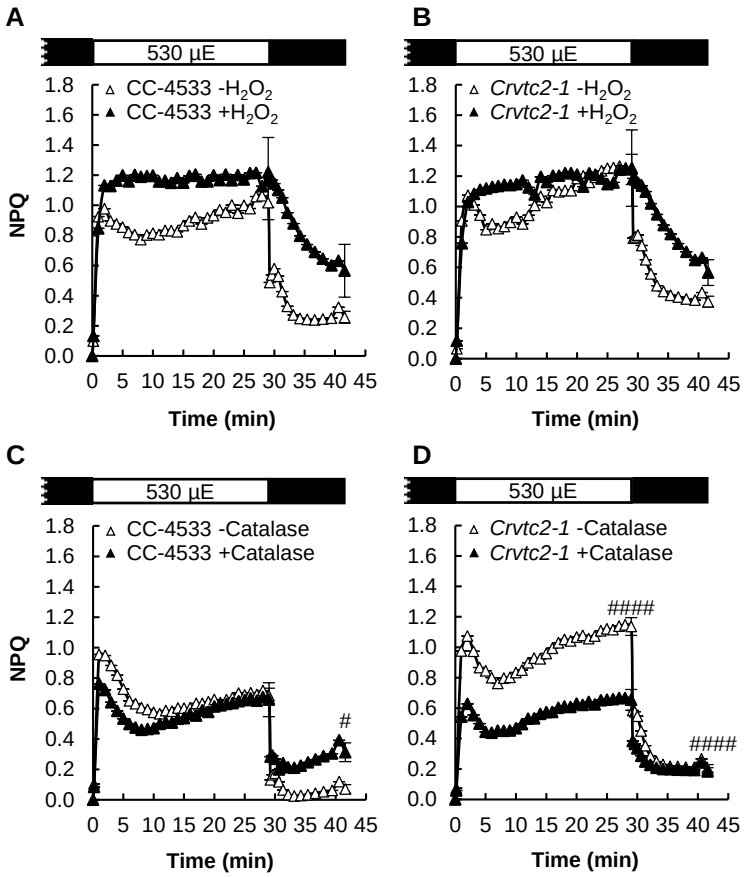

Figure 8 – The effects of H_2O_2 and catalase on NPQ induced by strong red light (530 µmol photons m^{-2} s^{-1}) in the wild-type (CC-4533) and *Crvtc2-1* mutant strains grown photoautotrophically in HS medium at 530 µmol photons m^{-2} s^{-1}. A, The effect of 1.5 mM H_2O_2 on NPQ induction in the CC-4533 strain; B, the effect of 1.5 mM H_2O_2 on NPQ induction in the *Crvtc2-1* mutant; C, the effect of catalase on NPQ induction in the CC-4533 strain; D, the effect of catalase on NPQ induction in the *Crvtc2-1* mutant. The presented data are based on four independent experiments. When applicable, averages and standard errors (±SE) were calculated. Data were analyzed by one-way ANOVA followed by Dunnett's post-test: # p<0.05, #### p<0.0001 compared to the untreated CC-4533 culture at the respective time-point. µE stands for µmol photons m^{-2} s^{-1}.

Parsed Citations

Adams WW III, Muller O, Cohu CM, Demmig-Adams B (2013) May photoinhibition be a consequence, rather than a cause, of limited plant productivity? Photosynth Res 117:31-44

Pubmed: Author and Title
Google Scholar: Author Only Title Only Author and Title

Allorent G, Tokutsu R, Roach T, Peers G, Cardol P, Girard-Bascou J, Seigneurin-Berny D, Petroutsos D, Kuntz M, Breyton C, Franck F, Wollman FA, Niyogi KK, Krieger-Liszkay A, Minagawa J, Finazzi G (2013) A dual strategy to cope with high light in Chlamydomonas reinhardtii. Plant Cell 25:545-557

Pubmed: Author and Title
Google Scholar: Author Only Title Only Author and Title

Anwaruzzaman M, Chin BL, Li X-P, Lohr M, Martinez DA, Niyogi KK (2004) Genomic analysis of mutants affecting xanthophyll biosynthesis and regulation of photosynthetic light harvesting in Chlamydomonas reinhardtii. Photosynth Res 82:265-276

Pubmed: Author and Title
Google Scholar: Author Only Title Only Author and Title

Arnoux P, Morosinotto T, Saga G, Bassi R, Pignol D (2009) A structural basis for the pH-dependent xanthophyll cycle in Arabidopsis thaliana. Plant Cell 21: 2036-2044

Pubmed: Author and Title
Google Scholar: Author Only Title Only Author and Title

Asada K (2006) Production and scavenging of reactive oxygen species in chloroplasts and their functions. Plant Physiol 141: 391-396

Pubmed: Author and Title
Google Scholar: Author Only Title Only Author and Title

Avenson TJ, Ahn TK, Zigmantas D, Niyogi KK, Li Z, Ballottari M, Bassi R, Fleming GR (2008) Zeaxanthin radical cation formation in minor light-harvesting complexes of higher plant antenna. J Biol Chem 283:3550-3558

Pubmed: Author and Title
Google Scholar: Author Only Title Only Author and Title

Azzabi G, Pinnola A, Betterle N, Bassi R, Alboresi A (2012) Enhancement of non-photo de-epoxidation index chemical quenching in the bryophyte Physcomitrella patens during acclimation to salt and osmotic stress. Plant Cell Physiol 53: 1815-1825

Pubmed: Author and Title
Google Scholar: Author Only Title Only Author and Title

Barahimipour R, Strenkert D, Neupert J, Schroda M, Merchant SS, Bock R (2015) Dissecting the contributions of GC content and codon usage to gene expression in the model alga Chlamydomonas reinhardtii. Plant J 84: 704-717

Pubmed: Author and Title
Google Scholar: Author Only Title Only Author and Title

Baroli I, Do AD, Yamane T, Niyogi KK (2003) Zeaxanthin accumulation in the absence of a functional xanthophyll cycle protects Chlamydomonas reinhardtii from photooxidative stress. Plant Cell 15: 992-1008

Pubmed: Author and Title
Google Scholar: Author Only Title Only Author and Title

Bratt C, Arvidsson P, Carlsson M, Akerlund H (1995) Regulation of violaxanthin de-epoxidase activity by pH and ascorbate. Photosynth Res 45: 169-175

Pubmed: Author and Title
Google Scholar: Author Only Title Only Author and Title

Bonente G, Ballottari M, Truong T, Morosinotto T, Ahn T, Fleming G, Niyogi K, Bassi R (2011) Analysis of LhcSR3, a protein essential for feedback de- excitation in the green alga Chlamydomonas reinhardtii. PLoS Biol 9:e1000577

Pubmed: Author and Title
Google Scholar: Author Only Title Only Author and Title

Bradbury LMT, Shumskaya M, Tzfadia O, Wu S-B, Kennelly EK, Wurtzelt ET (2012) Lycopene cyclase paralog CruP protects against reactive oxygen species in oxygenic photosynthetic organisms. Proc Natl Acad Sci USA 109:E1888-E1897

Pubmed: Author and Title
Google Scholar: Author Only Title Only Author and Title

Chaux F, Johnson X, Auroy P, Beyly-Adriano A, Te I, Cuiné S, Peltier G (2017) PGRL1 and LHCSR3 compensate for each other in controlling photosynthesis and avoiding photosystem I photoinhibition during high light acclimation of Chlamydomonas cells. Mol Plant 10:216-218

Pubmed: Author and Title
Google Scholar: Author Only Title Only Author and Title

Christa G, Cruz S, Jahns P, de Vries J, Cartaxana P, Esteves AC, Serôdio J, Gould SB (2017) Photoprotection in a monophyletic branch of chlorophyte algae is independent of energy-dependent quenching (qE). New Phytol 214: 1132-1144

Pubmed: Author and Title
Google Scholar: Author Only Title Only Author and Title

Depège N, Bellafiore S, Rochaix JD (2003) Role of chloroplast protein kinase Stt7 in LHCII phosphorylation and state transition in

Chlamydomonas. Science 299: 1572-1575
Pubmed: Author and Title
Google Scholar: Author Only Title Only Author and Title

Dowdle J, Ishikawa T, Gatzek S, Rolinski S, Smirnoff N (2007) Two genes in Arabidopsis thaliana encoding GDP-L-galactose phosphorylase are required for ascorbate biosynthesis and seedling viability. Plant J 52: 673-689
Pubmed: Author and Title
Google Scholar: Author Only Title Only Author and Title

Erickson E, Wakao S, Niyogi KK (2015) Light stress and photoprotection in Chlamydomonas reinhardtii. Plant J 82:449-465
Pubmed: Author and Title
Google Scholar: Author Only Title Only Author and Title

Fernie AR, Tóth SZ (2015) Identification of the elusive chloroplast ascorbate transporter extends the substrate specificity of the PHT family. Mol Plant 8:674-676
Pubmed: Author and Title
Google Scholar: Author Only Title Only Author and Title

Finazzi G, Johnson GN, Dall'Osto L, Zito F, Bonente G, Bassi R, Wollman F-A (2006) Nonphotochemical quenching of chlorophyll fluorescence in Chlamydomonas reinhardtii. Biochemistry 45:1490-1498
Pubmed: Author and Title
Google Scholar: Author Only Title Only Author and Title

Foyer CH, Shigeoka S (2011) Understanding oxidative stress and antioxidant functions to enhance photosynthesis. Plant Physiol 155: 93-100
Pubmed: Author and Title
Google Scholar: Author Only Title Only Author and Title

Gest N, Gautier H, Stevens R (2013) Ascorbate as seen through plant evolution: the rise of a successful molecule? J Exp Bot 64:33-53
Pubmed: Author and Title
Google Scholar: Author Only Title Only Author and Title

Grouneva I, Jakob T, Wilhelm C, Goss R (2006) Influence of ascorbate and pH on the activity of the diatom xanthophyll cycle-enzyme diadinoxanthin de-epoxidase. Physiol Plant 126:205-211
Pubmed: Author and Title
Google Scholar: Author Only Title Only Author and Title

Hager A, Holocher K (1994) Localization of the xanthophyll-cycle enzyme violaxanthin de-epoxidase within the thylakoid lumen and abolition of its mobility by a (light-dependent) pH decrease. Planta 192: 581-589
Pubmed: Author and Title
Google Scholar: Author Only Title Only Author and Title

Hallin EI, Hasan M, Guo K, Åkerlund H-E (2016) Molecular studies on structural changes and oligomerisation of violaxanthin de-epoxidase associated with the pH-dependent activation. Photosynth Res 129: 29-41
Pubmed: Author and Title
Google Scholar: Author Only Title Only Author and Title

Hieber AD, Bugos RC, Yamamoto HY (2000) Plant lipocalins: violaxanthin de-epoxidase and zeaxanthin epoxidase. Biochim Biophys Acta BBA - Protein Struct Mol Enzymol 1482: 84-91
Pubmed: Author and Title
Google Scholar: Author Only Title Only Author and Title

Holt NE, Zigmantas D, Valkunas L, Li X-P, Niyogi KK, Fleming GR (2005) Carotenoid cation formation and the regulation of photosynthetic light harvesting. Science 307:433-436
Pubmed: Author and Title
Google Scholar: Author Only Title Only Author and Title

Holub O, Seufferheld MJ, Gohlke C, Heiss GJ, Clegg RM (2007) Fluorescence lifetime imaging microscopy of Chlamydomonas reinhardtii: non-photochemical quenching mutants and the effect of photosynthetic inhibitors on the slow chlorophyll fluorescence transient. J Microsc 226: 90-120
Pubmed: Author and Title
Google Scholar: Author Only Title Only Author and Title

Ivanov B, Asada K, Edwards GE (2007) Analysis of donors of electrons to photosystem I and cyclic electron flow by redox kinetics of P700 in chloroplasts of isolated bundle sheath strands of maize. Photosynth Res 92:65-74
Pubmed: Author and Title
Google Scholar: Author Only Title Only Author and Title

Iwai M, Kato N, Minagawa J (2007) Distinct physiological responses to a high light and low CO2 environment revealed by fluorescence quenching in photoautotrophically grown Chlamydomonas reinhardtii. Photosynth Res 94:307-314
Pubmed: Author and Title
Google Scholar: Author Only Title Only Author and Title

Jeffrey SW, Mantoura RFC, Wright SW (1997) Phytoplankton pigments in oceanography: guidelines to modern methods. (Paris: UNESCO Publishing)

Pubmed: Author and Title
Google Scholar: Author Only Title Only Author and Title

Johnson X, Alric J (2012) Interaction between starch breakdown, acetate assimilation, and photosynthetic cyclic electron flow in Chlamydomonas reinhardtii. J Biol Chem 287:26445-26452
Pubmed: Author and Title
Google Scholar: Author Only Title Only Author and Title

Johnson MP, Davison PA, Ruban AV, Horton P (2008) The xanthophyll cycle pool size controls the kinetics of non-photochemical quenching in Arabidopsis thaliana. FEBS Lett 582:259-263
Pubmed: Author and Title
Google Scholar: Author Only Title Only Author and Title

Kanazawa A, Kramer DM (2002). In vivo modulation of nonphotochemical exciton quenching (NPQ) by regulation of the chloroplast ATP synthase. Proc Natl Acad Sci USA 99:12789-12794
Pubmed: Author and Title
Google Scholar: Author Only Title Only Author and Title

Kovács L, Vidal-Meireles A, Nagy V, Tóth SZ (2016) Quantitative determination of ascorbate from the green alga Chlamydomonas reinhardtii by HPLC. Bio-Protoc 6:e2067
Pubmed: Author and Title
Google Scholar: Author Only Title Only Author and Title

Lemeille S, Willig A, Depège-Fargeix N, Delessert C, Bassi R, Rochaix J-D (2009) Analysis of the chloroplast protein kinase Stt7 during state transitions. PLoS Biol 7: e1000045
Pubmed: Author and Title
Google Scholar: Author Only Title Only Author and Title

Li S, Liu L, Zhuang X, Yu Y, Liu X, Cui X, Ji L, Pan Z, Cao X, Mo B, Zhang F, Raikhel N, Jiang L, and Chen X (2013) MicroRNAs inhibit the Ttranslation of target mRNAs on the endoplasmic reticulum in Arabidopsis. Cell 153: 562-574
Pubmed: Author and Title
Google Scholar: Author Only Title Only Author and Title

Li Z, Peers G, Dent RM, Bai Y, Yang SY, Apel W, Leonelli L, Niyogi KK (2016a) Evolution of an atypical de-epoxidase for photoprotection in the green lineage. Nat Plants 2: 16140
Pubmed: Author and Title
Google Scholar: Author Only Title Only Author and Title

Li X, Zhang R, Patena W, Gang SS, Blum SR, Ivanova N, Yue R, Robertson JM, Lefebvre PA, Fitz-Gibbon ST, Grossman AR, Jonikas MC (2016b) An indexed, mapped mutant library enables reverse genetics studies of biological processes in Chlamydomonas reinhardtii. Plant Cell 28: 367-387
Pubmed: Author and Title
Google Scholar: Author Only Title Only Author and Title

Marschall M, Proctor MCF (2004) Are bryophytes shade plants? Photosynthetic light responses and proportions of chlorophyll a, chlorophyll b and total carotenoids. Ann Bot 94: 593-603
Pubmed: Author and Title
Google Scholar: Author Only Title Only Author and Title

Müller-Moulé P, Conklin PL, Niyogi KK (2002) Ascorbate deficiency can limit violaxanthin de-epoxidase activity in vivo. Plant Physiol 128: 970-977
Pubmed: Author and Title
Google Scholar: Author Only Title Only Author and Title

Müller-Moulé P, Havaux M, Niyogi KK (2003) Zeaxanthin deficiency enhances the high light sensitivity of an ascorbate-deficient mutant of Arabidopsis. Plant Physiol 133: 748-760.
Pubmed: Author and Title
Google Scholar: Author Only Title Only Author and Title

Nagy V, Vidal-Meireles A, Podmaniczki A, Szentmihályi K, Rákhely G, Zsigmond L, Kovács L, Tóth SZ (2018) The mechanism of photosystem II inactivation during sulphur deprivation-induced H2 production in Chlamydomonas reinhardtii. Plant J 94:548-561
Pubmed: Author and Title
Google Scholar: Author Only Title Only Author and Title

Neupert J, Karcher D, Bock R (2009) Generation of Chlamydomonas strains that efficiently express nuclear transgenes. Plant J 57:1140-1150
Pubmed: Author and Title
Google Scholar: Author Only Title Only Author and Title

Niyogi KK, Bjorkman O, Grossmann AR (1997) Chlamydomonas xanthophyll cycle mutants identified by video imaging of chlorophyll fluorescence quenching. Plant Cell 9:1369-1380
Pubmed: Author and Title
Google Scholar: Author Only Title Only Author and Title

Peers G, Truong TB, Ostendorf E, Busch A, Elrad D, Grossman AR, Hippler M, Niyogi KK (2009) An ancient light-harvesting protein is

critical for the regulation of algal photosynthesis. Nature 462:518-521
Pubmed: Author and Title
Google Scholar: Author Only Title Only Author and Title

Pinnola A, Dall'Osto L, Gerotto C, Morosinotto T, Bassi R, Alboresi A (2013) Zeaxanthin binds to Light-Harvesting Complex Stress-Related Protein to enhance nonphotochemical quenching in Physcomitrella patens. Plant Cell 25:3519-3534
Pubmed: Author and Title
Google Scholar: Author Only Title Only Author and Title

Polukhina I, Fristedt R, Dinc E, Cardol P, Croce R (2016) Carbon supply and photoacclimation cross talk in the green alga Chlamydomonas reinhardtii. Plant Physiol 172: 1494-1505
Pubmed: Author and Title
Google Scholar: Author Only Title Only Author and Title

Porra RJ, Thompson WA, Kriedeman PE (1989) Determination of accurate extinction coefficients and simultaneous equations for essaying chlorophylls-a and -b with four different solvents: verification of the concentration of chlorophyll standards by atomic absorption spectroscopy. Biochim Biophys Acta 975: 384-394
Pubmed: Author and Title
Google Scholar: Author Only Title Only Author and Title

Quaas T, Berteotti S, Ballottari M, Flieger K, Bassi R, Wilhelm C, Goss R (2015) Non-photochemical quenching and xanthophyll cycle activities in six green algal species suggest mechanistic differences in the process of excess energy dissipation. J. Plant Physiol 172: 92-103
Pubmed: Author and Title
Google Scholar: Author Only Title Only Author and Title

Roach T, Na CS (2017) LHCSR3 affects de-coupling and re-coupling of LHCII to PSII during state transitions in Chlamydomonas reinhardtii. Sci Rep 7: 43145
Pubmed: Author and Title
Google Scholar: Author Only Title Only Author and Title

Ruban AV, Johnson MP, Duffy CD (2012) The photoprotective molecular switch in the photosystem II antenna. Biochim Biophys Acta 1817:167-181
Pubmed: Author and Title
Google Scholar: Author Only Title Only Author and Title

Saga G, Giorgetti A, Fufezan C, Giacometti GM, Bassi R, Morosinotto T (2010) Mutation analysis of violaxanthin de-epoxidase identifies substrate-binding sites and residues involved in catalysis. J Biol Chem 285:23763-23770
Pubmed: Author and Title
Google Scholar: Author Only Title Only Author and Title

Schroda M, Vallon O, Whitelegge JP, Beck CF, Wollman FA (2001) The chloroplastic GrpE homolog of Chlamydomonas: two isoforms generated by differential splicing. Plant Cell 13:2823-2839
Pubmed: Author and Title
Google Scholar: Author Only Title Only Author and Title

Smirnoff N (2018) Ascorbic acid metabolism and functions: A comparison of plants and mammals. Free Radic Biol Med. 122:116-129
Pubmed: Author and Title
Google Scholar: Author Only Title Only Author and Title

Takizawa K, Kanazawa A, Kramer DM (2008) Depletion of stromal Pi induces high 'energy dependent' antenna exciton quenching (qE) by decreasing proton conductivity at CFO-CF1 ATP synthase. Plant Cell Environ 31:235-243
Pubmed: Author and Title
Google Scholar: Author Only Title Only Author and Title

Tibiletti T, Auroy P, Peltier G, Caffarri S (2016) Chlamydomonas reinhardtii PsbS protein is functional and accumulates rapidly and transiently under high light. Plant Physiol 171:2717-2730
Pubmed: Author and Title
Google Scholar: Author Only Title Only Author and Title

Tikkanen M, Mekala NR, Aro E-M (2014) Photosystem II photoinhibition-repair cycle protects photosystem I from irreversible damage. Biochim Biophys Acta - Bioenerg 1837: 210-215
Pubmed: Author and Title
Google Scholar: Author Only Title Only Author and Title

Tóth SZ, Puthur JT, Nagy V, Garab G (2009) Experimental evidence for ascorbate-dependent electron transport in leaves with inactive oxygen-evolving complexes. Plant Physiol 149: 1568-1578
Pubmed: Author and Title
Google Scholar: Author Only Title Only Author and Title

Tóth SZ, Nagy V, Puthur JT, Kovács L, Garab G (2011) The physiological role of ascorbate as photosystem II electron donor: Protection against photoinactivation in heat-stressed leaves. Plant Physiol 156: 382-392
Pubmed: Author and Title
Google Scholar: Author Only Title Only Author and Title

Tóth SZ, Lőrincz T, Szarka A (2018) Concentration does matter: The beneficial and potentially harmful effects of ascorbate in humans and plants. Antioxid Redox Signal 29:1516-1533
Pubmed: Author and Title
Google Scholar: Author Only Title Only Author and Title

Ünlü C, Drop B, Croce R, van Amerongen H (2014) State transitions in Chlamydomonas reinhardtii strongly modulate the functional size of photosystem II but not of photosystem I. Proc Natl Acad Sci USA 111:3460-3465
Pubmed: Author and Title
Google Scholar: Author Only Title Only Author and Title

Urzica EI, Adler LN, Page MD, Linster CL, Arbing MA, Casero D, Pellegrini M, Merchant SS, Clarke SG (2012) Impact of oxidative stress on ascorbate biosynthesis in Chlamydomonas via regulation of the VTC2 gene encoding a GDP-L-galactose phosphorylase. J Biol Chem 287: 14234-14245
Pubmed: Author and Title
Google Scholar: Author Only Title Only Author and Title

Vidal-Meireles A, Neupert J, Zsigmond L, Rosado-Souza L, Kovács L, Nagy V, Galambos A, Fernie AR, Bock R, Tóth SZ (2017) Regulation of ascorbate biosynthesis in green algae has evolved to enable rapid stress-induced response via the VTC2 gene encoding GDP- L -galactose phosphorylase. New Phytol 214: 668-681
Pubmed: Author and Title
Google Scholar: Author Only Title Only Author and Title

Voigt J, Münzner P (1994) Blue light-induced lethality of a cell wall-deficient mutant of the unicellular green alga Chlamydomonas reinhardtii. Plant Cell Physiol 35: 99-106
Pubmed: Author and Title
Google Scholar: Author Only Title Only Author and Title

Wang Z, Xiao Y, Chen W, Tang K, Zhang L (2010) Increased vitamin C content accompanied by an enhanced recycling pathway confers oxidative stress tolerance in Arabidopsis. J. Integr. Plant Biol 52: 400-409
Pubmed: Author and Title
Google Scholar: Author Only Title Only Author and Title

Wheeler G, Ishikawa T, Pornsaksit V, Smirnoff N (2015) Evolution of alternative biosynthetic pathways for vitamin C following plastid acquisition in photosynthetic eukaryotes. eLife 4:e06369
Pubmed: Author and Title
Google Scholar: Author Only Title Only Author and Title

Xue H, Tokutsu R, Bergner SV, Scholz M, Minagawa J, Hippler M (2015) Photosystem II subunit R is required for efficient binding of Light-Harvesting Complex Stress-Related Protein 3 to photosystem II-light-harvesting supercomplexes in Chlamydomonas reinhardtii. Plant Physiol 167: 1566-1578
Pubmed: Author and Title
Google Scholar: Author Only Title Only Author and Title

Zechmann B, Stumpe M, Mauch F (2011) Immunocytochemical determination of the subcellular distribution of ascorbate in plants. Planta 233: 1-12
Pubmed: Author and Title
Google Scholar: Author Only Title Only Author and Title